Title

A Cdc48 “Retrochaperone” Function Is Required for the Solubility of Retrotranslocated, Integral Membrane Endoplasmic Reticulum-associated Degradation (ERAD-M) Substrates* * This work was supported by National Institutes of Health Grant 5R37DK051996-1...

Journal

Journal of Biological Chemistry, 292(8)

ISSN

0021-9258

Authors

Neal, Sonya

Mak, Raymond

Bennett, Eric J

et al.

Publication Date

2017-02-01

DOI

10.1074/jbc.m116.770610

THE JOURNAL OF BIOLOGICAL CHEMISTRY VOL. 292, NO. 8, pp. 3112–3128, February 24, 2017

A Cdc48 "Retrochaperone" Function Is Required for the Solubility of Retrotranslocated, Integral Membrane Endoplasmic Reticulum-associated Degradation (ERAD-M) Substrates*

Received for publication, December 1, 2016, and in revised form, January 10, 2017 Published, JBC Papers in Press, January 11, 2017, DOI 10.1074/jbc.M116.770610

Sonya Neal, Raymond Mak, Eric J. Bennett, and Randolph Hampton[1]

From the Division of Biological Sciences, Section of Cell and Developmental Biology, University of California, San Diego, La Jolla, California 92093

Edited by George N. DeMartino

A surprising feature of endoplasmic reticulum (ER)-associated degradation (ERAD) is the movement, or retrotranslocation, of ubiquitinated substrates from the ER lumen or membrane to the cytosol where they are degraded by the 26S proteasome. Multispanning ER membrane proteins, called ERAD-M substrates, are retrotranslocated to the cytosol as full-length intermediates during ERAD, and we have investigated how they maintain substrate solubility. Using an *in vivo* assay, we show that retrotranslocated ERAD-M substrates are moved to the cytoplasm as part of the normal ERAD pathway, where they are part of a solely proteinaceous complex. Using proteomics and direct biochemical confirmation, we found that Cdc48 serves as a critical "retrochaperone" for these ERAD-M substrates. Cdc48 binding to retrotranslocated, ubiquitinated ERAD-M substrates is required for their solubility; removal of the polyubiquitin chains or competition for binding by addition of free polyubiquitin liberated Cdc48 from retrotranslocated proteins and rendered them insoluble. All components of the canonical Cdc48 complex Cdc48-Npl4-Ufd1 were present in solubilized ERAD-M substrates. This function of the complex was observed for both HRD and DOA pathway substrates. Thus, in addition to the long known ATP-dependent extraction of ERAD substrates during retrotranslocation, the Cdc48 complex is generally and critically needed for the solubility of retrotranslocated ERAD-M intermediates.

Endoplasmic reticulum (ER)[2]-associated degradation (ERAD) refers to a group of quality control pathways that degrade damaged or misfolded ER-localized proteins (1, 2). ERAD occurs through the ubiquitin-proteasome pathway, by which ubiquitin is attached to ERAD substrates to cause proteasomal degradation (3–5). Specifically, multiple copies of ubiquitin are transferred from an E2 ubiquitin-conjugating enzyme (UBC) to the target protein by an E3 ubiquitin ligase, forming multiubiquitin chains that are recognized by the 26S proteasome followed by ATP-dependent unfolding and degradation of the substrate (6). ERAD is responsible for degradation of a variety of misfolded proteins, including both fully luminal (ERAD-L) and integral membrane (ERAD-M) substrates (7, 8). ERAD pathways can also degrade a number of normal proteins; the best studied is the essential enzyme HMGR (HMG-CoA reductase). In both yeast and mammals, HMGR undergoes regulated ERAD as part of cellular control of sterol synthesis. In mammals, the lone HMGR enzyme is subject to regulated ERAD; in yeast, the Hmg2 isozyme undergoes regulated degradation, and the Hmg1 isozyme is stable in all conditions (2, 9).

In *Saccharomyces cerevisiae*, ERAD is mediated by the HRD (HMG-CoA Reductase Degradation) and DOA (Degradation of α 2) pathways, both of which are conserved in all eukaryotes (1, 2, 4, 11). In the HRD pathway, the multispanning integral membrane E3 ubiquitin ligase Hrd1 mediates the degradation of numerous substrates, including the normal Hmg2 isozyme (12, 13). In the DOA pathway, the distinct multispanning integral membrane E3 ligase Doa10 ubiquitinates a large and mostly distinct group of misfolded soluble and membrane proteins, often containing cytosolic determinants of Doa10 recognition (5).

ERAD pathways present the cell with a spatial challenge. The 26S proteasome resides in the cytosol and connected compartments, along with the E1 ubiquitin-activating enzyme and most E2s. Accordingly, a unifying feature of all ERAD pathways is the requirement for movement of substrates from the ER membrane or lumen to the cytosol for degradation. This transport component of ERAD is broadly referred to as dislocation or retrotranslocation, and it has been known to occur since the earliest studies of ERAD, when it was realized that cytosolic

* This work was supported by National Institutes of Health Grant 5R37DK051996-18 (to R. H.), National Institutes of Health Postdoctoral Fellowship 1F32GM111024-01 (to S. N.), and Burroughs Wellcome Fund 1013987 (to S. N.) and DP2GM119132 (to E. J. B). The authors declare that they have no conflicts of interest with the contents of this article. The content is solely the responsibility of the authors and does not necessarily represent the official views of the National Institutes of Health.

We dedicate this work to the memory of the remarkable Stefan Jentsch, who was a vibrant and ultra-creative scientist as well as a generous, humorous, and unique colleague. You will be missed.

[1] To whom correspondence should be addressed: University of California, San Diego, 9500 Gilman Dr., La Jolla, CA 92093-0347. Tel.: 858-822-0511; Fax: 858-534-0555; E-mail: rhampton@ucsd.edu.

[2] The abbreviations used are: ER, endoplasmic reticulum; ERAD, ER-associated degradation; HMGR, HMG-CoA reductase; Ub, ubiquitin; GGPP, geranylgeranyl pyrophosphate; Co-IP, coimmunoprecipitation; S, supernatant; P, pellet; NEM, *N*-ethylmaleimide; IPB, immunoprecipitation buffer; IP, immunoprecipitation; PI, protease inhibitor.

Ubc7 was responsible for the ubiquitin-mediated degradation of luminal ERAD substrate CPY* (14, 15). Since then, many studies have confirmed the general importance of this process in all ERAD pathways (15–18).

Despite intense efforts in studying ERAD, the mechanism(s) and machinery of retrotranslocation remain poorly understood. A unifying feature of retrotranslocation is the requirement of the ATPase Cdc48 (p97 in mammals) as an energy source for substrate removal or extraction from the ER membrane. Cdc48 consists of an N-terminal domain, two ATPase ring domains (D1 and D2), and a C-terminal tail, and it is normally hexameric (19). In ERAD, Cdc48 is bound to the substrate-binding cofactors Ufd1-Npl4 via its N-terminal domain (20–22). The proteins Ufd1 and Npl4 form a complex with the Cdc48 hexamer, allowing for recognition and binding of ubiquitinated substrates and their extraction from the ER membrane. ATP hydrolysis catalyzed by the Cdc48 AAA ATPase D1 and D2 domains powers this extraction process (19, 23). Malfunction of Cdc48/p97 in recognizing ubiquitinated substrates blocks the retrotranslocation process (16, 24), and aberrant accumulation of retrotranslocation substrates has been linked to various neurodegenerative diseases such as Alzheimer's, rheumatoid arthritis, and cancer (25). Intriguingly, the retrotranslocation step itself is employed to activate the transcription factor and ERAD substrate Nrf1 by movement of a luminal proteolytic site to a cytosolic protease, resulting in activation by cleavage (26). Thus, the nature of retrotranslocated ERAD substrates holds great interest in understanding both normal and pathophysiological processes that involve these pathways. Of particular interest is the physical state of retrotranslocated material. Especially for multispanning membrane proteins, the question of how these molecules can be rendered soluble, and the factors or biomolecules that allow stable solubility of these substrates, is an important and open question.

To explore these questions, we focused on the eponymous canonical HRD pathway substrate Hmg2, the ERAD-regulated isozyme of HMGR. Hmg2 is an eight transmembrane-span ER-resident membrane protein that can undergo rapid degradation by the HRD pathway (2, 9). Using an *in vitro* HRD-dependent ubiquitination assay, we had previously demonstrated HRD- and Cdc48-dependent retrotranslocation of full-length Hmg2 to the cytosol where it exists in a soluble form (16). In the work below, we studied the physical and biochemical state of retrotranslocated Hmg2, in order to understand this poorly characterized segment of the ERAD pathway. We developed a physiologically relevant *in vivo* retrotranslocation assay to directly examine this degradation intermediate in intact cells, and we have done both biophysical and proteomic studies on *in vivo* retrotranslocated Hmg2. We found that retrotranslocated Hmg2 was not associated with lipids but rather was associated with protein. Proteomics were used to discover proteins associated with retrotranslocated Hmg2; the most consistent and highest abundance Hmg2 retrochaperone was Cdc48. Biochemical studies confirmed the proteomic results case and showed that all soluble, retrotranslocated Hmg2 was associated with the Cdc48-Ufd1-Npl4 complex. Furthermore, association of Cdc48 with retrotranslocated Hmg2 was required for its stable solubility after retrotranslocation. Finally, this finding was extended to the other principal ERAD pathway, Doa10. Similar to Hmg2, the canonical ERAD-M substrate of Doa10, the multispanning integral membrane substrate Ste6* (also called Ste6-166), was quantitatively associated with Cdc48 when solubilized by retrotranslocation. These results indicate a universal and critical role for the Cdc48 complex in both the movement and the solubility of ERAD-M clients during their destruction in the living cell.

Results

In Vitro Retrotranslocated Hmg2 Is Not Lipid-associated—To gain an understanding of retrotranslocation, we wanted to determine the physical state of retrotranslocated membrane proteins, and the molecules involved in maintaining them in the soluble state. Our laboratory had developed a biologically relevant *in vitro* retrotranslocation assay using the normally degraded and regulated ERAD-M substrate Hmg2-GFP (16). The *in vitro* retrotranslocation assay consists of preparing microsomes from a strain devoid of the main HRD E2 (Ubc7) but expressing the E3 ligase Hrd1 and ERAD-M substrate Hmg2-GFP. These microsomes are mixed with cytosol from cells not expressing Hmg2-GFP but expressing the missing E2 Ubc7 to initiate *in vitro* HRD-dependent ubiquitination and retrotranslocation of Hmg2-GFP. After a reaction period, the entire mixture is centrifuged for 1 h at 20,000 $\times$ *g* to discern retrotranslocated, ubiquitinated Hmg2-GFP present in the soluble fraction (S20) from the portion of ubiquitinated Hmg2 that remains in the membrane (P20). The ubiquitinated Hmg2-GFP in each fraction is assayed by solubilization and immunoprecipitation with anti-GFP antibodies, followed by SDS-PAGE and immunoblotting for ubiquitinated material (α-Ub) or Hmg2-GFP (α-GFP) (Fig. 1*A*). As described previously, the soluble ubiquitinated Hmg2 is the portion that has been retrotranslocated and remains soluble even after ultracentrifugation at 100,000 $\times$ *g* (see below) (16). Soluble retrotranslocated Hmg2-GFP is full length, and it can be recovered as such by stripping off the attached ubiquitin with ubiquitin protease Usp2 catalytic core (Usp2Core, Fig. 1*B*). Importantly, *in vitro* Hmg2-GFP retrotranslocation requires functional Cdc48, as demonstrated by using a strain with the *cdc48-3* hypomorph as the source of microsomes or cytosol. In this assay, the principal contribution is from the cytosol, but use of both *cdc48-2* microsomes and cytosol causes complete block of retrotranslocation (Fig. 1*C*). Furthermore, hydrolysis of the γ-phosphate bond of ATP (note: ubiquitination requires the α-bond) and the Hrd1-dependent ubiquitination of the Hmg2-GFP substrate are both required for retrotranslocation as well (16). Fig. 1, *A–C,* recapitulates the *in vitro* retrotranslocation assay as characterized in detail previously (16). We used this assay as a starting point for understanding the biochemical nature of retrotranslocated ERAD-M substrates.

We suspected that specific proteins, which we term "retrochaperones," are required for the surprising solubility of retrotranslocated full-length Hmg2-GFP, as has been shown for the Ste6* (also called Ste6-166) DOA10 pathway substrate (27). Nevertheless, it remained formally possible that lipids were involved in solubilizing Hmg2 by formation of micelles and/or lipid droplet-like particles (28, 29). To address this, we isolated

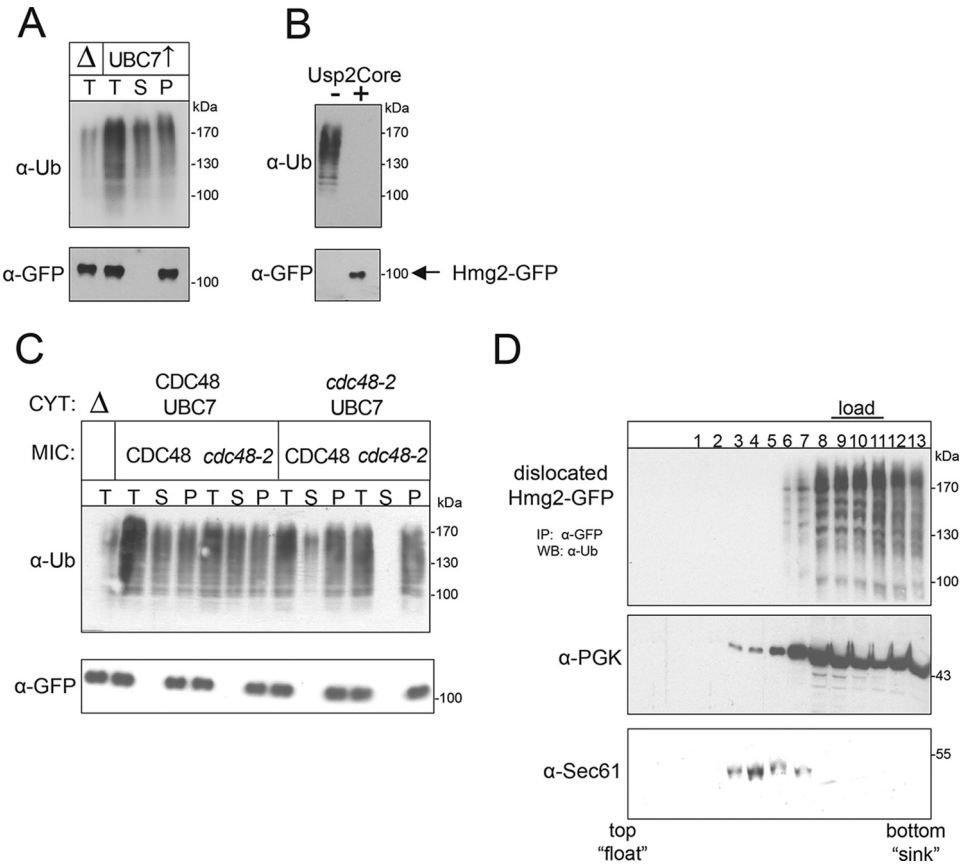

FIGURE 1. ***In vitro* retrotranslocated Hmg2 does not associate with lipids.** *A, in vitro* retrotranslocation of Hmg2-GFP. Microsomes were prepared from Δ*hrd1* strains expressing $TDH3_{pr}$-Hmg2-GFP and $TDH3_{pr}$-Hrd1. Cytosol was prepared from strains expressing $TDH3_{pr}$-UBC7 or no Ubc7 (Δ*ubc7*). To initiate ubiquitination and retrotranslocation of Hmg2-GFP, microsomes and cytosol were mixed, and the reaction was centrifuged to discern ubiquitinated Hmg2-GFP that either has been retrotranslocated into the S20 S or remained in the membrane P20 P. *T*, total. Following fractionation, Hmg2-GFP was immunoprecipitated from both fractions, resolved on 8% SDS-PAGE, and immunoblotted for ubiquitin or Hmg2-GFP. *B,* full-length Hmg2-GFP retrotranslocated *in vitro*. Supernatant fraction isolated from *in vitro* retrotranslocation assay as described above was incubated with buffer or Usp2Core for 1 h at 37 °C. Full-length Hmg2-GFP was immunoprecipitated and immunoblotted for ubiquitin or Hmg2-GFP. *C, in vitro* retrotranslocation of Hmg2-GFP required Cdc48. *In vitro* retrotranslocation was a carried out as described above. Different combinations of WT of *cdc48-2* prepared from microsomes (*MIC*) and cytosol (*CYT*) were mixed to evaluate the Cdc48 contribution to Hmg2-GFP retrotranslocation. *D, in vitro* retrotranslocated Hmg2-GFP does not associate with lipids. Crude lysate or S100 supernatant containing retrotranslocated Hmg2-GFP was prepared, layered at the bottom of the centrifuge tube, and subjected to ultracentrifugation as described under "Experimental Procedures." Aliquots were removed from the top to the bottom of the sucrose gradient, and each fraction was directly immunoblotted for Sec61 and PGK with anti-Sec61 or anti-PGK, respectively, or immunoprecipitated with anti-GFP and immunoblotted for ubiquitinated Hmg2-GFP with anti-ubiquitin. *WB*, Western blot.

in vitro retrotranslocated Hmg2-GFP and analyzed it by ultracentrifugal flotation to evaluate its association with lipids. Briefly, the supernatant (S20) from the *in vitro* retrotranslocation assay, containing ubiquitinated soluble Hmg2-GFP, was mixed with a dense sucrose solution (2.4 M), placed in a centrifuge tube, and overlaid with steps of sucrose solutions of progressively lower densities (Fig. 1*D*). This tube was then subjected to overnight ultracentrifugation to evaluate hydrodynamic properties of the retrotranslocated Hmg2-GFP. Fractions were removed across the gradient, immunoprecipitated with anti-GFP antibodies, and immunoblotted for ubiquitination to ascertain the position in the gradient of retrotranslocated Hmg2-GFP. Various control proteins were also evaluated in the gradients by immunoblotting the same fractions to establish the veracity of the buoyancy analysis (Fig. 1*D*). The soluble cytoplasmic enzyme PGK remained in the lower fractions (7–13), whereas the membrane-associated ER-resident integral membrane protein Sec61 floated to higher fractions (4–6). The retrotranslocated Hmg2-GFP showed mobility coincident with PGK suggesting that *in vitro* retrotranslocated Hmg2-GFP is not associated with lipids; rather, it appeared to be proteinaceous. To further explore this idea, we next developed an *in vivo* assay for higher physiological veracity.

In Vivo Hmg2-GFP Retrotranslocation Assay—The above studies indicated that soluble retrotranslocated Hmg2-GFP was not associated with lipids. This was observed in the *in vitro* assay, which is powerful and highly accessible for manipulation of reaction conditions, but it employs overexpressed Hrd1 to drive the reaction (16). Both sterol pathway regulation and the absolute requirement for Hrd3 observed *in vivo* are lost *in vitro*. In addition, the effects of null mutations in the post-ubiquitination adaptors Rad23 and Dsk2 cause an *in vitro* block to retrotranslocation not predicted by *in vivo* studies (16). Accordingly, to study Hmg2 in a more physiological context, we developed an *in vivo* retrotranslocation assay, based on earlier work on ERAD-L substrates (30). Untreated intact cells in which Hmg2-GFP was undergoing sterol pathway-dependent degradation were lysed without detergent, and lysates were ultracentrifuged to separate membrane-bound from retrotranslocated, ubiquitinated Hmg2-GFP. After ultracentrifuga-

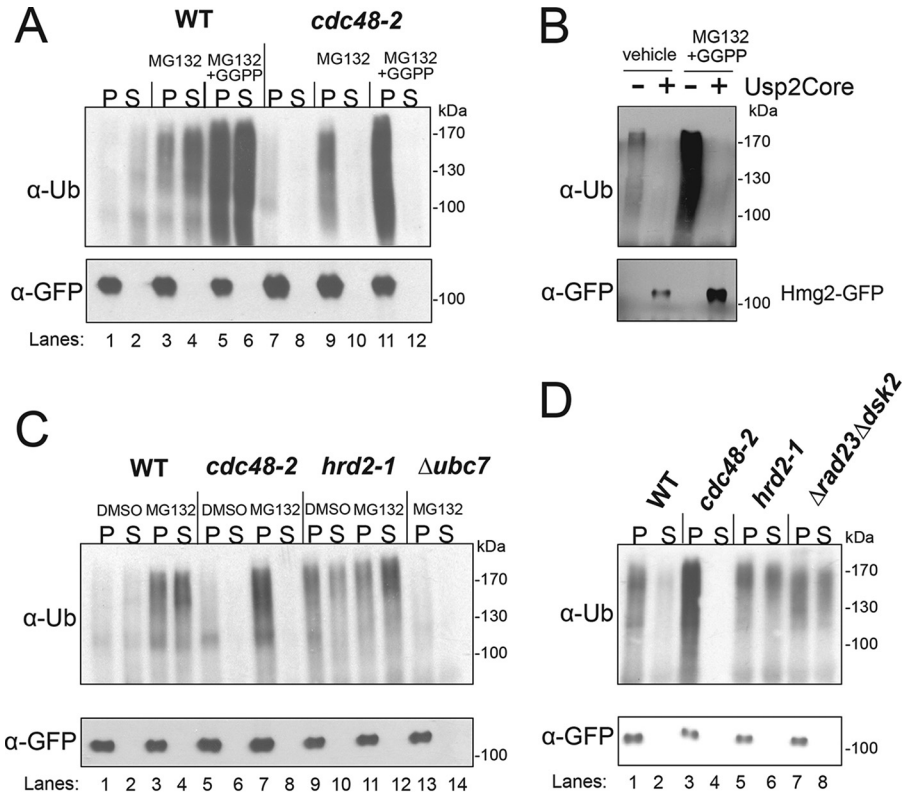

FIGURE 2. ***In vivo* retrotranslocated soluble Hmg2-GFP was full length.** *A,* GGPP induced ubiquitination and retrotranslocation of Hmg2-GFP. WT and *cdc48-2* strains were grown to log phase and treated with different combinations of MG132 (25 μg/ml) and GGPP (11 μM). Crude lysate was prepared from each strain and ultracentrifuged to discern ubiquitinated Hmg2-GFP that either has been retrotranslocated into the soluble fraction (S) or remained in the membrane (P). Following fractionation, Hmg2-GFP was immunoprecipitated from both fractions, resolved on 8% SDS-PAGE, and immunoblotted for ubiquitin and Hmg2-GFP. *B,* full-length Hmg2-GFP retrotranslocates into soluble fraction *in vivo*. S100 supernatant containing retrotranslocated Hmg2-GFP was isolated from *in vivo* retrotranslocation assay and incubated in the presence or absence of Usp2Core for 1 h at 37 °C. Full-length Hmg2-GFP was immunoprecipitated and immunoblotted for ubiquitin or Hmg2-GFP. *C, in vivo* retrotranslocation of Hmg2-GFP requires Cdc48. Same as *A* except WT, *cdc48-2*, *hrd2-1,* and Δ*ubc7* were used and treated with vehicle or MG132 (25 μg/ml). *D, in vivo* retrotranslocation of Hmg2-GFP does not require proteasome shuttle factors Rad23/Dsk2. Same experiment as *C* except Δ*rad23*Δ*dsk2* strain was included.

tion, ubiquitinated Hmg2-GFP was immunoprecipitated from the S fraction using anti-GFP antibodies and was detected by ubiquitin immunoblotting. The pellet was solubilized and analyzed by anti-GFP IP and immunoblotting as well. As expected from the *in vitro* results, a substantial fraction of the ubiquitinated Hmg2-GFP was soluble (Fig. 2*A*, *lanes 1* and *2*). This indicated that there was an extant ambient level of soluble retrotranslocated material en route to the proteasome in normal conditions. Consistent with this idea, addition of proteasome inhibitor MG132 caused a buildup of ubiquitinated Hmg2-GFP in both the P and S fraction, because ubiquitination and retrotranslocation could proceed to a larger extent when the proteasome was blocked (Fig. 2*A*, *lanes 3* and *4*).

Use of the *in vivo* assay preserved sterol pathway regulation of Hmg2 stability. As shown previously, the 20-carbon sterol pathway molecule geranylgeranyl pyrophosphate (GGPP) is an endogenous regulator of Hmg2-GFP that stimulates increased Hmg2 ubiquitination and degradation (31). Addition of GGPP to cells along with proteasome inhibitors caused further increased ubiquitination of Hmg2-GFP and increased appearance of ubiquitinated Hmg2-GFP in the S fraction (Fig. 2*A*, *lanes 5* and *6*). In all these conditions, retrotranslocated, ubiquitinated Hmg2-GFP was only found in the S fraction when Cdc48 was functional; strains with the *cdc48-2* hypomorphic allele showed a nearly complete block in retrotranslocation of Hmg2-GFP in all three conditions (untreated, MG132, and MG132 + GGPP) but no effect on the extent of total ubiquitination caused by the additions (Fig. 2*A*, *lanes 7–12*).

We confirmed that the ubiquitinated Hmg2-GFP in the *in vivo* assay supernatant was full length by stripping the immunoprecipitated material with the Usp2Core ubiquitin protease and blotting for GFP after SDS-PAGE; full-length Hmg2-GFP was recovered in the soluble fraction (Fig. 2*B*) in both untreated cells and those with maximal signal due to treatment with MG132 and GGPP.

We further characterized the *in vivo* retrotranslocation assay by examining the effects of a variety of ERAD mutants, using *cdc48-2* as a positive control (Fig. 2*C*, *lanes 5–8*). The historic ERAD mutant *hrd2-1* is an allele of the 26S proteasome base subunit Rpn1 that is strikingly deficient in Hmg2 degradation (13). As expected, in an *hrd2-1* strain, there was increased total ubiquitination of Hmg2-GFP and more accumulation in the soluble fraction compared with WT. Moreover, the signal intensity in each fraction was greater still when MG-132 was added to the *hrd2-1* strain due to further inhibition of the proteasome (Fig. 2*C*, *lanes 9–12*). In cells lacking Ubc7, the principal HRD pathway E2 (30), Hmg2-GFP was not ubiquitinated, and so no retrotranslocated Hmg2-GFP was generated (Fig. 2*C*, *lanes 13* and *14*). Finally, previous *in vivo* studies implicated a set of adaptor proteins Rad23 and Dsk2 for facilitating transfer

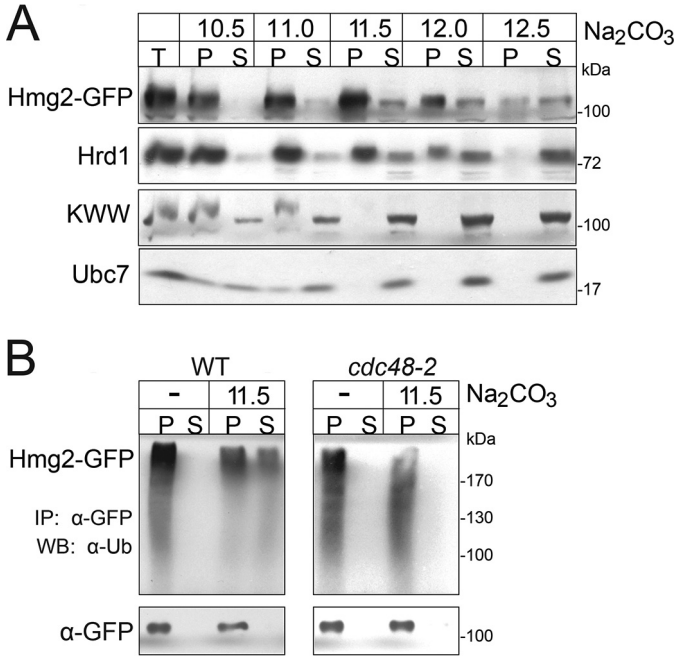

FIGURE 3. **Cdc48 is required for extraction of ubiquitinated Hmg2-GFP from the ER membrane.** *A,* microsomes were analyzed by alkali extraction (Na_2CO_3) with 0.2 M carbonate at the indicated pH values. Equal volumes of the P and TCA-precipitated S fractions were resolved by SDS-PAGE and analyzed by immunoblotting. *B,* for analysis of ubiquitinated Hmg2-GFP, pellet and supernatant fractions were immunoprecipitated for Hmg2-GFP and immunoblotted for ubiquitinated Hmg2-GFP with anti-Ub.

of ubiquitinated ERAD substrates to the proteasome (33, 34). In double null cells lacking both Rad23 and Dsk2, there was a predicted greater percentage of ubiquitinated Hmg2-GFP in the soluble fraction compared with WT, and no block in retrotranslocation (Fig. 2*D*). Taken together, these characterization studies indicated that the *in vivo* assay adhered to the current model of ERAD-M removal from the ER membrane (16, 17, 35). The retrotranslocation of full-length Hmg2-GFP occurred normally during Hrd-dependent degradation, and both ubiquitination and functional Cdc48 were required for Hmg2-GFP retrotranslocation, whereas the proteolysis and Rad23/Dsk2 were involved in steps downstream of membrane extraction. We proceeded with our studies on the nature of retrotranslocated Hmg2-GFP using this high fidelity *in vivo* assay.

Ubiquitinated mammalian HMGR has been reported to collect on the surface of the ER pending movement to the proteasome (36). Accordingly, we tested the degree to which ubiquitinated and membrane-associated Hmg2-GFP had retained its integral protein status. We asked whether any of the ER-associated, ubiquitinated Hmg2-GFPs were similarly tightly bound to the outer ER surface and thus extractable by chemical means. To discern integral membrane, ubiquitinated Hmg2-GFP from surface-bound material, we used carbonate (CO_3^{2-}) extraction over the pH range 10.5 to 12.5, because integral membrane proteins are far less extractable than extrinsic ones (Fig. 3*A*) (37). Pellet fractions from strains expressing Hmg2-GFP or control proteins were subject to treatment with 0.2 M $Na_2CO_3^{2-}$ carbonate buffers at the indicated pH values and then were centrifuged and analyzed by immunoblotting to evaluate liberation by the treatment. The majority of integral membrane protein Hrd1 remained in the pellet until pH 12–12.5. Tail-anchored protein KWW and non-covalently anchored (via Cue1) E2 Ubc7 showed similar intermediate patterns remaining mostly in the pellet until pH 11.5. Like Hrd1, non-ubiquitinated Hmg2-GFP remained in the pellet fraction until a pH above 12, as expected from its eight-spanning anchor. In striking contrast, ubiquitinated Hmg2-GFP that was pellet-associated show a substantial fraction that was liberated at pH 11.5, ~30% of the total membrane-associated material (Fig. 3*B*). The presence of this surface-bound retrotranslocated Hmg2-GFP was fully dependent on active Cdc48; in an identical experiment in a *cdc48-2* mutant, no ubiquitinated Hmg2-GFP was extracted from the pellet at the same pH. Taken together, these studies show that the retrotranslocation of full-length ubiquitinated Hmg2-GFP occurs at normal levels of all HRD components and is part of degradation over the broad range of half-lives possible with this regulated substrate. Furthermore, Cdc48 is required for the initial removal of ubiquitinated Hmg2 from the ER membrane, rather than extraction from a surface-bound pool that has undergone retrotranslocation.

In Vivo Retrotranslocated Hmg2-GFP Is Not Lipid-associated—The *in vitro* retrotranslocation assay clearly shows that soluble ubiquitinated Hmg2-GFP is not lipid-associated. We next performed the same analysis on retrotranslocated Hmg2-GFP produced in the newly characterized *in vivo* assay. Cells were treated with the proteasome inhibitor MG132 and Hmg2 degradation regulator GGPP to maximize retrotranslocated material. After lysis and ultracentrifugation, the S100 supernatant bearing soluble retrotranslocated Hmg2-GFP was subjected to sucrose density gradient analysis as above (Fig. 4), again using soluble PGK and integral ER-membrane protein Sec61 as gradient controls. As expected, PGK remained in the lower fractions, whereas membrane-associated Sec61 and ER-localized and ubiquitinated Hmg2-GFP (from the P fraction of the retrotranslocation assay) floated to higher fractions (2, 4–9), as expected for integral membrane proteins. Conversely, the distribution of retrotranslocated, ubiquitinated Hmg2-GFP from the S fraction coincided with PGK indicating that *in vivo* retrotranslocated Hmg2-GFP consisted of protein and was not lipid-associated.

Multispanning DOA Pathway Substrate Ste6 Behaves Identically to HRD Substrate Hmg2-GFP*—A recent study by Nakatsukasa and Kamura (27) was conducted on the physical state of retrotranslocated integral membrane ERAD substrate Ste6*-3HA (also called Ste6-166-3HA), which is degraded by the distinct DOA pathway through the action of the Doa10 E3 ligase. Although Ste6*-3HA is also a multispanning integral membrane protein, its biochemical behavior after retrotranslocation was reported to be different from our observations of Hmg2-GFP, in what appeared to be a very similar assay. Unlike retrotranslocated Hmg2 in our studies (see above) (16), retrotranslocated Ste6*-3HA that was soluble in a 20,000 × *g* spin (in the S20 fraction) was reported to be fully precipitated upon further centrifugation at 100,000 × *g*. This observation suggested an intermediate of retrotranslocated Ste6*-3HA that was not completely soluble. Because the downstream segments of the HRD and DOA pathways are thought to converge on retrotranslocation, a difference between these apparently similar substrates

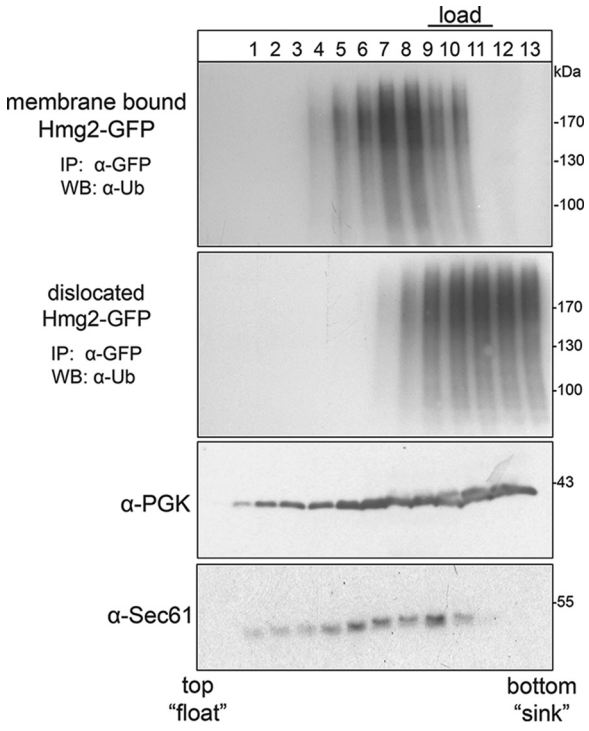

FIGURE 4. ***In vivo* retrotranslocated Hmg2 does not associate with lipids.** Crude lysate or S100 supernatant and P100 pellet were prepared, layered at the bottom of a centrifuge tube, and subjected to ultracentrifugation as described under "Experimental Procedures." Aliquots were removed from the top to the bottom of the sucrose gradient, and each fraction was either directly immunoblotted for Sec61 and PGK with anti-Sec61 or anti-PGK, respectively, or immunoprecipitated with anti-GFP and immunoblotted for ubiquitin and Hmg2-GFP. *WB,* Western blot.

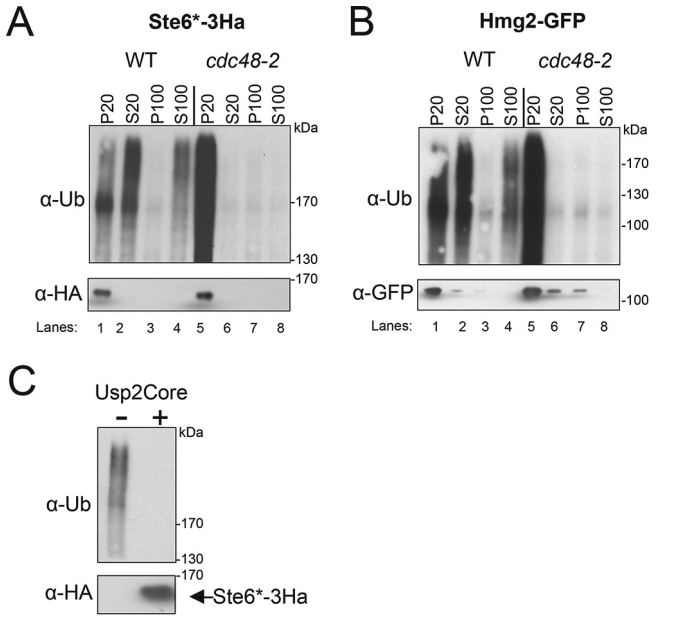

FIGURE 5. **Ste6-166 retrotranslocates identically as Hmg2-GFP.** *A,* retrotranslocated Ste6* remains soluble in the S100 fraction. Crude lysate from WT and *cdc48-2* strains expressing Ste6*-3HA were centrifuged at 20,000 × *g* at 4 °C to yield membrane fraction (P20) and supernatant fraction (S20). S20 supernatant was further ultracentrifuged at 100,000 × *g* at 4 °C to yield membrane fraction (P100) and supernatant fraction (S100). Ste6*-3HA was immunoprecipitated from all fractions with anti-HA (Covance), resolved on 8% SDS-PAGE, and immunoblotted with anti-HA for Ste6*-3HA or anti-ubiquitin for ubiquitinated Ste6*-3HA. Retrotranslocated Hmg2-GFP remains in the S100 fraction. *B,* same as *A* except WT and *cdc48-2* strains expressing Hmg2-GFP were used instead. *C,* full-length Ste6* retrotranslocates into the S100 fraction. S100 supernatant was incubated in the presence or absence of Usp2Core for 1 h at 37 °C. Ste6*-3HA was immunoprecipitated with polyclonal anti-HA and immunoblotted with anti-HA and anti-Ub.

could be an important clue about differences in retrotranslocation mechanisms used in these distinct ERAD pathways. Accordingly, we included this DOA substrate to directly compare retrotranslocation of Hmg2-GFP and Ste6*-3HA in our assay (Fig. 5, *A* and *B*). Upon centrifugation at 20,000 × *g*, similar fractions of retrotranslocated, ubiquitinated Hmg2-GFP or Ste6*-3HA were found in the soluble fraction (S20) (Fig. 5, *A*, *lane 2,* and *B, lane 2*). However, in our assay, when the S20 fraction was then ultracentrifuged at 100,000 × *g*, both ubiquitinated Hmg2-GFP and Ste6*-3HA remained completely soluble (S100), showing no enrichment in the pellet fraction (P100) (Fig. 5, *A*, *lane 4,* and *B*, *lane 4*). As expected, in retrotranslocation-deficient *cdc48-2* cells, both substrates remained in the pellet fraction (P20) (Fig. 5, *A*, *lanes 5–8,* and *B*, *lanes 5–8*). Importantly, removal of ubiquitin from the soluble Ste6*-3HA with Usp2Core led to recovery of the full-length 12 membrane spanning protein (S100; Fig. 5*C*). Thus, as far as we can tell, the two pathway substrates behave in an identical manner in our *in vivo* retrotranslocation assay, such that complete Cdc48-dependent removal of each full-length substrate from the ER membrane to a soluble form appears to occur. We also observed the same behavior for Ste6*-3HA-GFP (data not shown). We next endeavored to understand the proteins that allow solubility of retrotranslocated multispanning ERAD-M substrates.

Proteomic Analysis of Proteins Associated with Retrotranslocated Hmg2-GFP—Our observation of retrotranslocated Hmg2-GFP being protein-associated demanded analysis of the accompanying proteins that allow an eight-spanning ERAD-M substrate to exist in a soluble and unaggregated state. To identify these potential retrochaperones, we used an unbiased proteomics approach. We maximized the amount of retrotranslocated material in the S fraction by treating with proteasome inhibitor MG132 and degradation stimulus GGPP, and we increased the number of cells used to 30 OD units. The ultracentrifuged S fraction was subjected to preparative anti-GFP coimmunoprecipitation (Co-IP) using GFP-Trap affinity beads in the absence of detergent to capture retrotranslocated, ubiquitinated Hmg2-GFP and any associated proteins. As controls, Co-IPs was performed on S fractions from otherwise identical strains not expressing Hmg2-GFP and strains expressing cytosolic GFP. Following Co-IP, low pH eluted proteins were digested with trypsin and subjected to LC-MS/MS analysis. We performed mass spectrometry-based analysis of retrotranslocated Hmg2-GFP association three independent times. The first two were done with more stringent IP conditions (Fig. 6*A* and Table 1), whereas the last sample was isolated using conditions that favored more weakly associated candidates (data not shown). We identified a number of proteins that interacted with Hmg2-GFP (as defined by ≥1.5-fold enrichment over control IPs (Fig. 6*A* and Table 1). Notably, the hexameric ATPase Cdc48 emerged as the most prominent protein associated with retrotranslocated Hmg2-GFP in all replicates compared with control IPs (highlighted in *red*; Fig. 6*A*). In addition to the Cdc48, we identified other Hmg2-GFP-interacting proteins,

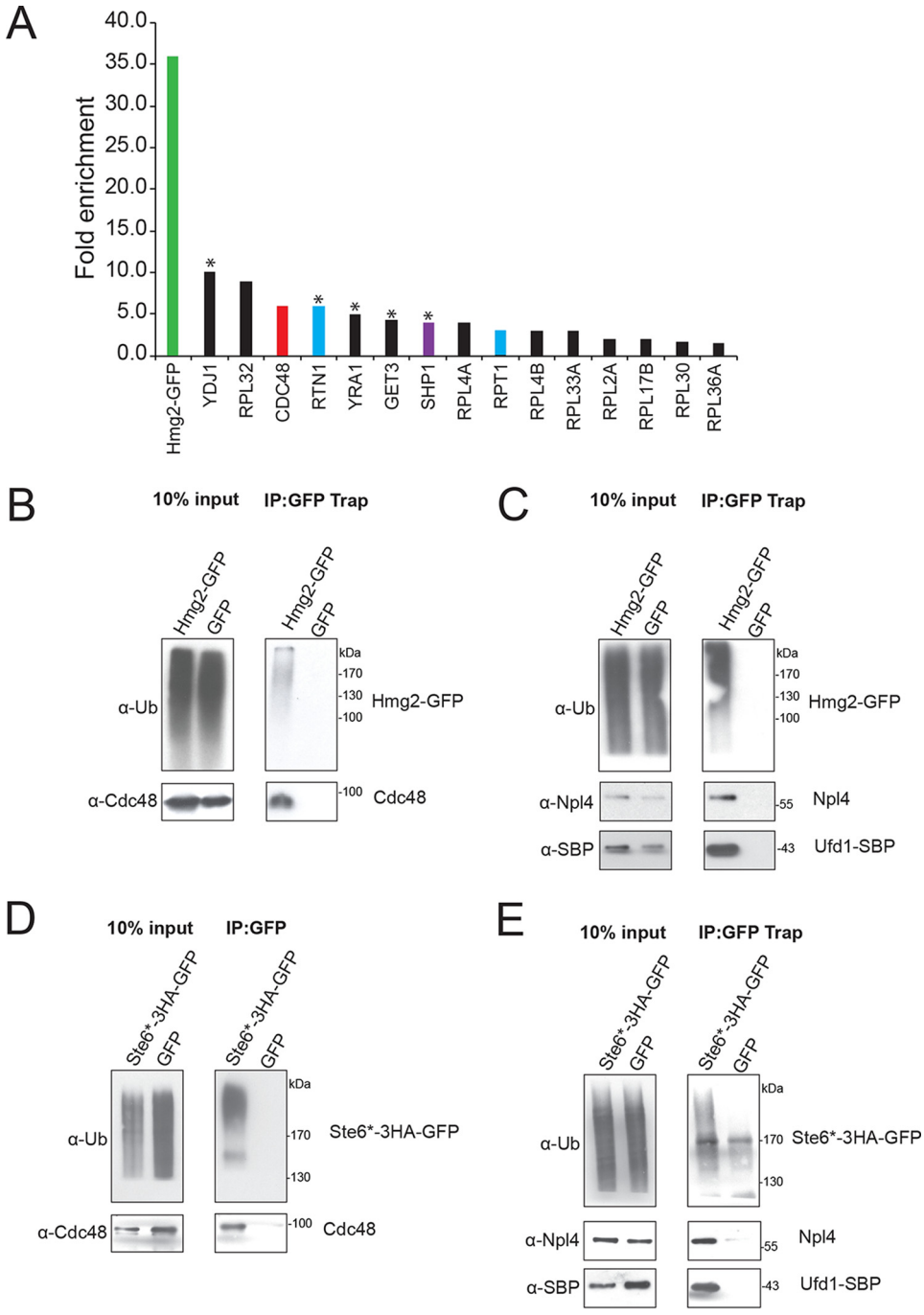

FIGURE 6. **Cdc48 is the main interacting protein of retrotranslocated Hmg2-GFP.** *A,* S100 supernatant containing retrotranslocated Hmg2-GFP and control strains not expressing Hmg2-GFP or expressing cytosolic GFP were precipitated with GFP-Trap beads. Following Co-IP, low pH-eluted proteins were digested with trypsin and subjected to LC-MS/MS analysis. A representative *bar graph* from the first two runs of mass spectrometry analysis was generated to include fold enrichment for corresponding proteins, which reflects the relative enrichment of spectral counts for interacting proteins *versus* the beads only and cytosolic GFP control. Proteins with ≥1.5-fold enrichment over controls in the mass spectra were included. Note: Hmg2-GFP is highlighted in *green*; Cdc48 is highlighted in *red*; proteasome subunits are highlighted *blue,* and Cdc48 cofactors are highlighted in *purple*. *B,* Hmg2-GFP Co-IPs with Cdc48. Strains expressing the indicated proteins were grown, and equal amounts were harvested. S100 supernatant was prepared as described under "Experimental Procedures" and immunoprecipitated with GFP-Trap to pull down retrotranslocated Hmg2-GFP. The precipitates were resolved on 8% SDS-PAGE and immunoblotted for ubiquitinated Hmg2-GFP and Cdc48. *C,* Hmg2-GFP Co-IPs with Npl4 and Ufd1. Same as *B* except Hmg2-GFP precipitates were resolved on 8% SDS-PAGE and immunoblotted for Npl4 and Ufd1. *D,* Ste6*-3HA-GFP Co-IPs with Cdc48. Same as *B* except strains expressing Ste6*-3HA-GFP were used for immunoprecipitation with GFP-Trap followed by immunoblotting for Cdc48. *E,* same as *D* except Ste6*-3HA-GFP precipitates were resolved and immunoblotted for Npl4 and Ufd1-SBP.

including known components of the ubiquitin proteasome pathway. These included the Cdc48 cofactor (highlighted in *purple*) and components of the 20S proteasome (highlighted in *blue*) (Fig. 6*A*). Some intriguing candidate Hmg2-GFP-interacting proteins were identified in only a subset of replicate experiments (Fig. 6*A*, marked by *asterisks*), including Get3, a member of the Get complex known to interact with tail-anchored proteins to ferry their hydrophobic cargos to the ER

TABLE 1
Spectral counts and fold enrichment for proteins identified from LC–MS/MS analysis
Fold enrichment = (Hmg2-GFP$^{s.c.}$)/(beads only$^{s.c.}$ + GFP$^{s.c.}$), s.c. is spectral counts.

Gene	Total Peptides Identified	beads only	GFP	HMG2-GFP	Fold Enrichment
HMG2	36	0	0	36	36.0
YDJ1	11	0	1	10	10.0
RPL32	20	0	2	18	9.0
CDC48	6	0	0	6	6.0
RTN1	6	0	0	6	6.0
YRA1	6	0	1	5	5.0
GET3	16	2	1	13	4.3
SHP1	4	0	0	4	4.0
RPL4A	15	3	0	12	4.0
RPT1	3	0	0	3	3.0
RPL4B	12	3	0	9	3.0
RPL33A	8	1	1	6	3.0
RPL2A	24	4	4	16	2.0
RPL17B	32	6	5	21	1.9
RPL30	8	0	3	5	1.7
RPL36A	25	6	4	15	1.5

surface while avoiding the indignity of aggregation. These results indicate a number of candidates involved in retrochaperoning Hmg2-GFP, which we directly tested in the biochemical studies below.

Cdc48 as an ERAD-M Retrochaperone—We investigated the highest ranking candidates from the proteomic studies to discern the factors directly involved in Hmg2-GFP retrotranslocation (Fig. 6*A*). We confirmed an interaction between Cdc48 and retrotranslocated Hmg2-GFP. After preparation of S100 as above, retrotranslocated Hmg2-GFP was immunoprecipitated by GFP-Trap Co-IP in non-detergent conditions, and affinity-purified material was directly analyzed by immunoblotting. A substantial fraction of Cdc48 (~10% of input) co-purified with retrotranslocated Hmg2-GFP, whereas no Cdc48 co-purified with immunoprecipitated cytosolic GFP (Fig. 6*B*).

Cdc48 performs its known ERAD functions while associated with Npl4 and Ufd1 (20, 21). Ufd1, but not Npl4, was detected in the lower stringency proteomics experiment, although with substantially fewer spectral counts for this single copy component in comparison with the hexameric Cdc48. We used a strain expressing a Ufd1-streptavidin-binding peptide fusion (Ufd1-SBP) to confirm its association with retrotranslocated Hmg2-GFP. Upon anti-GFP precipitation of retrotranslocated Hmg2-GFP, coprecipitated Ufd1-SPB was detected with anti-Ufd1 antibody (Fig. 6*C*). Because Npl4 is also involved in Cdc48-dependent ERAD, we also directly tested it for association with retrotranslocated Hmg2-GFP. Retrotranslocated Hmg2-GFP was precipitated with GFP-Trap followed by immunoblotting with anti-Npl4 polyclonal antibody (Fig. 6*C*), clearly showing that Npl4 was also associated with retrotranslocated Hmg2-GFP despite its absence in the proteomics studies. Thus, each member of the Cdc48-Ufd1-Npl4 complex was bound to retrotranslocated Hmg2-GFP.

We next performed the same association studies on the DOA pathway ERAD-M substrate Ste6*-3HA-GFP. The GFP version of Ste6*-3HA behaved identically to Ste6*-3HA used in the studies above. Immunoprecipitation of retrotranslocated Ste6*-3HA-GFP with GFP-Trap beads similarly coprecipitated Cdc48 (Fig. 6*D*), as well as Ufd1-SPB or Npl4 (Fig. 6*E*). The above results implied a critical role for the Cdc48 complex as a general retrochaperone for ERAD-M substrates from both the HRD and DOA pathways.

If Cdc48 is important for allowing retrotranslocated Hmg2-GFP to remain soluble, then we would predict that all of the soluble Hmg2-GFP should be associated with Cdc48. To test this idea, we performed a reverse coprecipitation experiment, removing Cdc48 by precipitation, and evaluated both association of Hmg2-GFP and the degree to which the retrotranslocated Hmg2-GFP was cleared from the supernatant. We employed a functional N-terminal protein A fusion of Cdc48 (ProtA-Cdc48) to facilitate high affinity capture. We developed a strain expressing the ProtA-Cdc48 fusion as the only source of Cdc48 to ensure complete removal of Cdc48. Importantly, this strain was viable and not temperature-sensitive. Furthermore, Hmg2-GFP in the ProtA-Cdc48 strain was normally degraded and regulated (Fig. 7*B*). These tests all confirm that the ProtA fusion expressed as the sole form of Cdc48 was fully functional (Fig. 7*A*).

We used the strain expressing only ProtA-Cdc48 to evaluate the extent to which retrotranslocated Hmg2 is associated with Cdc48. The soluble lysates (S100 supernatant) from retrotranslocation assays run in the ProtA-Cdc48 strain or a control untagged Cdc48 strain were affinity-precipitated with IgG beads to clear the ProtA-Cdc48 and then blotted for Cdc48 itself or for coimmunoprecipitated Hmg2-GFP (Fig. 7*C*). To improve detection, we took advantage of the ability to collapse the ubiquitinated Hmg2-GFP immunoreactivity into a single band by pre-treatment with Usp2Core. The coprecipitation supernatant was also evaluated for unbound Cdc48 or Hmg2-GFP. As expected from the previous coprecipitation, retrotranslocated Hmg2-GFP was associated with the bead-bound ProtA-Cdc48 (Fig. 7*C*, *top row*). Moreover, *all* the soluble Hmg2-GFP was found in the bead pellet, with none remaining in the soluble fraction. The identical experiment with the

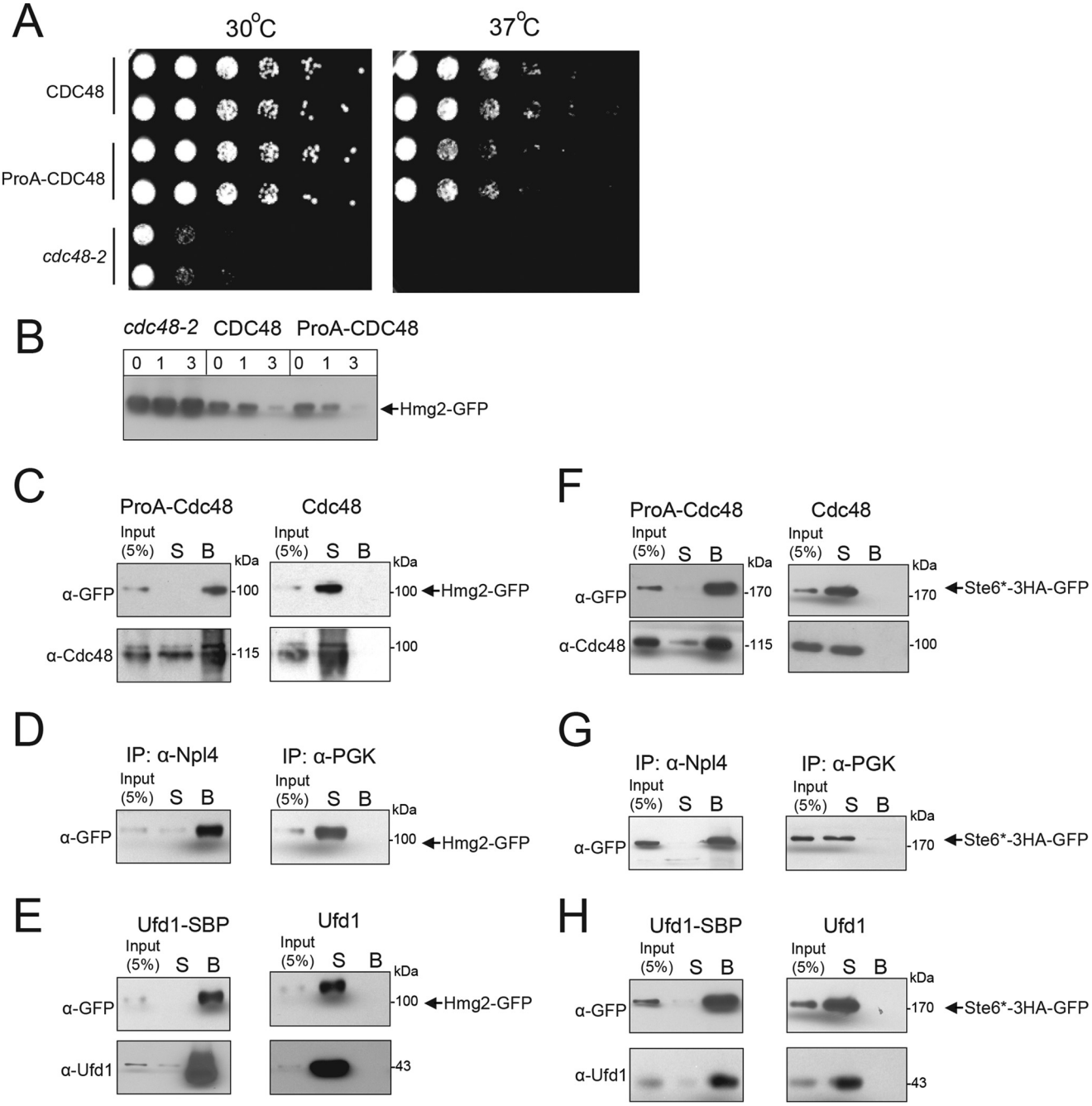

FIGURE 7. **All retrotranslocated Hmg2-GFP and Ste6-166 is bound to Cdc48 complex.** *A,* ProtA-Cdc48 complements endogenous Cdc48. Strains containing CDC48, ProtA-CDC48, or *cdc48-2* were compared for growth by dilution assay. Each strain was spotted at 5-fold dilutions on YPD, and plates were incubated at 30 and 37 °C. ProteinA-Cdc48 complements endogenous Cdc48 in ERAD of Hmg2-GFP. *B,* indicated strains expressing Hmg2-GFP were grown into log phase, and degradation was measured by a CHX chase. After CHX addition, cells were lysed at the indicated times and analyzed by SDS-PAGE and immunoblotting for Hmg2. *C,* strains expressing the indicated proteins were grown, and equal amounts were harvested. S100 supernatant was prepared as described under "Experimental Procedures" and immunoprecipitated with IgG-Sepharose to pull down ProtA-Cdc48. As a control, 5% of input was withdrawn, and the rest of the lysate was incubated with IgG-Sepharose. The Sepharose beads were washed, and bound proteins (*B*) were eluted with 2× USB. To assess the effectiveness of binding, the unbound S was also included. Samples were resolved on 8% SDS-PAGE and immunoblotted for Cdc48 with anti-Cdc48. Blotting for Hmg2-GFP with anti-GFP required treatment of all samples with Usp2Core prior to resolving on SDS-PAGE. *D,* same as *C* except S100 supernatant was immunoprecipitated with polyclonal anti-Npl4. As a control, polyclonal antibody against PGK was also used. Samples were resolved on 8% SDS-PAGE and immunoblotted for Hmg2-GFP with anti-GFP. *E,* same as *C* except S100 supernatant was immunoprecipitated with streptavidin beads to capture Ufd1-SBP. Samples were resolved on 8% SDS-PAGE and immunoblotted for Hmg2-GFP with anti-GFP and Ufd1-SBP with anti-Ufd1. *F,* same as *C* except Ste6*-3HA-GFP was analyzed for immunoprecipitation with ProtA-Cdc48. *G,* S100 supernatant was immunoprecipitated with polyclonal anti-Npl4. As a control, polyclonal antibody against PGK was also used. Samples were resolved on 8% SDS-PAGE and immunoblotted for Ste6*-3HA-GFP with anti-GFP. *H,* same as *C* except S100 supernatant was immunoprecipitated with streptavidin beads to capture Ufd1-SBP. Samples were resolved on 8% SDS-PAGE and immunoblotted for Ste6*-3HA-GFP with anti-GFP and Ufd1-SBP with anti-Ufd1.

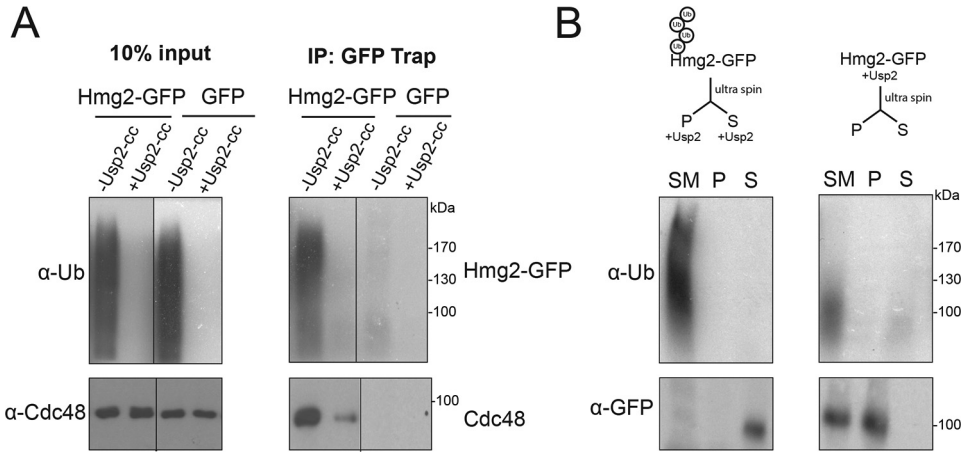

FIGURE 8. **Ubiquitin is required for Cdc48 association.** *A,* same as (Fig. 6) except GFP-Trap-captured retrotranslocated Hmg2-GFP was resuspended in 100 μl of XL buffer, treated with buffer or (5 μg) Usp2Core, and incubated for 1 h at 37 °C. GFP-Trap-agarose beads were washed twice with IPB buffer, washed once with IPW buffer, and aspirated to dryness. The precipitates were resuspended in 2× USB, resolved on 8% SDS-PAGE, and immunoblotted for ubiquitinated Hmg2-GFP and Cdc48. Hmg2 is no longer soluble upon removal of ubiquitin chains. *B, left panel*, S100 supernatant was prepared as described under "Experimental Procedures" and was ultracentrifuged to discern ubiquitinated Hmg2-GFP that is either in the insoluble fraction (*P*) or in the soluble fraction (*S*). Following ultracentrifugation, both P and S fractions were treated with Usp2Core, and Hmg2-GFP was immunoprecipitated from both fractions, resolved on 8% SDS-PAGE, and immunoblotted for ubiquitin and Hmg2-GFP. *Right panel*, same as above except Usp2Core was added to supernatant fraction prior to ultracentrifugation. *SM,* starting material.

untagged Cdc48 strain caused no capture of retrotranslocated Hmg2-GFP (Fig. 7*C*, *right panel*), such that it all remained soluble. It is worth noting that a variable portion of ProtA-Cdc48 does not precipitate with anti-IgG beads, whereas the Cdc48 that is bead-associated captures all of the Hmg2-GFP. In all likelihood, this small fraction of non-precipitated ProtA-Cdc48 is non-functional and misfolded, and so it does not bind to either IgG beads or retrotranslocated substrate. We similarly tested Npl4 or Ufd1 for the extent of retrotranslocated Hmg2-GFP association with these factors by the same approach. To test Npl4, a retrotranslocation S100 fraction was immunoprecipitated with polyclonal α-Npl4 antibodies. All of the retrotranslocated Hmg2-GFP were coprecipitated (Fig. 7*D*, *α-Npl4*), whereas none were captured when a control polyclonal antibody against PGK was used instead of anti-Npl4 (Fig. 7*D*, *α-PGK*). Similarly, an S100 fraction from a retrotranslocation assay performed on the Ufd1-SBP-expressing strain was precipitated with streptavidin beads to capture all of the Ufd1-SPB. Precipitation with streptavidin concomitantly caused complete clearance of all the retrotranslocated Hmg2-GFP (Fig. 7*E*, *Ufd1-SBP*), whereas an identical experiment from a strain with untagged Ufd1 captured no Hmg2-GFP (Fig. 7*E*, *Ufd1*).

We also tested retrotranslocated Doa10 substrate Ste6*-3HA-GFP for the degree of association with Cdc48 complex members. A ProtA-Cdc48 strain expressing Ste6*-3HA-GFP was subjected to the *in vivo* retrotranslocation assay and immunoprecipitation with IgG beads to capture Cdc48. The same results were observed as follows: removal of ProtA-Cdc48 specifically and completely removed retrotranslocated Ste6*-3HA-GFP from the supernatant (Fig. 7*F*), whereas no Ste6* was captured in an identical experiment in a strain with untagged Cdc48. Identical results were obtained in coprecipitation experiments with Npl4 or Ufd1-SPB (Fig. 7, *G* and *H*); full clearance of retrotranslocated Ste6* occurred by affinity precipitation of either factor. Taken together, these clearance experiments show that the Cdc48-Ufd1-Npl4 complex is quantitatively associated with retrotranslocated ERAD-M substrates from both major ERAD pathways, appropriate for a role in maintaining the solubility of ERAD-M substrates on their way to 26S destruction.

We examined a variety of other high scoring candidates from the proteomic analysis to evaluate their importance in retrotranslocation or degradation of Hmg2-GFP. This included Ydj1, Rtn1, Yra1, Get3, and Shp1 (indicated as *asterisks* in Fig. 6*A*). None of those tested, despite compelling roles in related processes, such as Get3 (38), showed any effect on Hmg2-GFP degradation. Taken together, upon dislocating from the ER, virtually all solubilized ERAD-M substrate is associated with the Cdc48 complex, indicating this hexamer is a major retrochaperone for solubilized ubiquitinated ERAD-M substrates. We next focused on the nature and function of its consistent and complete association with retrotranslocated ERAD-M substrates.

Nature and Function of Cdc48 Binding to Retrotranslocated Hmg2—Cdc48 binds to ubiquitinated proteins in a wide variety of circumstances (6, 24, 39, 40). The hexameric ATPase is thought to supply energy for removal of these substrates from membranes or proteinaceous complexes for eventual delivery to the proteasome or other cellular fates (41–43). Hence, Cdc48 has been termed a ubiquitin-dependent dislocase. The structure of the Npl4/Ufd1 subunits in the canonical Cdc48 complex includes polyubiquitin-binding sites that allow high affinity association with multiubiquitin chains (40). Because retrotranslocated Hmg2-GFP must be ubiquitinated to undergo this process, we explored the degree to which this critical modification was important for the interaction of soluble, retrotranslocated Hmg2-GFP with Cdc48. We first tested the effects of simply removing the chains on Hmg2-GFP/Cdc48 association. GFP-Trap precipitation was performed on retrotranslocated Hmg2-GFP, followed by ubiquitin stripping of the bead-captured substrate with Usp2Core ubiquitin protease to remove the covalently added ubiquitin (Fig. 8*A*). Removal of the mul-

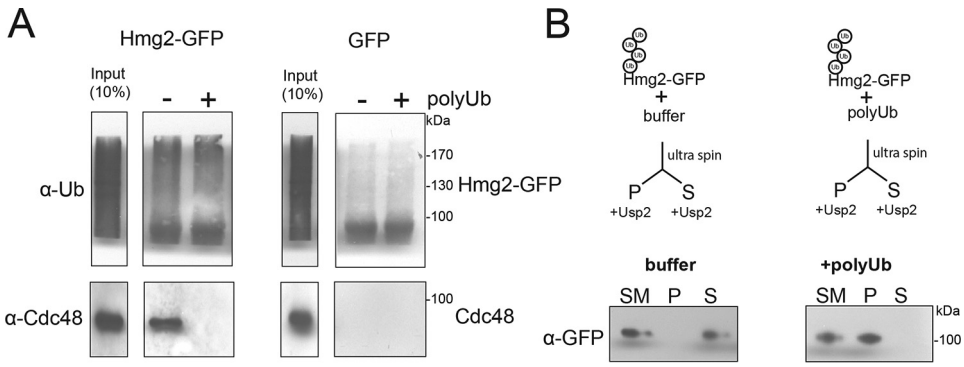

FIGURE 9. **Cdc48 is required for the solubility of Hmg2-GFP.** *A,* in the presence of Lys-48-linked polyubiquitin chains, Cdc48 disassociates from retrotranslocated Hmg2-GFP. Same as Fig. 6 except the S100 supernatant containing retrotranslocated Hmg2-GFP was treated with 5 μM Lys-48-linked polyubiquitin chains. *B,* retrotranslocated Hmg2-GFP is no longer soluble upon disassociation from Cdc48. Retrotranslocated Hmg2-GFP was treated with excess Lys-48-linked polyubiquitin chains or buffer and was ultracentrifuged to discern ubiquitinated Hmg2-GFP that is either in the insoluble fraction (*P*) or in the soluble fraction (*S*). Following ultracentrifugation, both P and S fractions were treated with Usp2Core.

tiubiquitin chains resulted in the release of ~90% of the bound Cdc48 from the bead-trapped Hmg2-GFP, indicating the expected function for attached ubiquitin in the association of Cdc48 with retrotranslocated Hmg2-GFP.

One hypothesis for Cdc48's role as a retrochaperone is that it is required for solubility of the retrotranslocated substrates. We next tested whether removal of the Cdc48 by ubiquitin stripping affects the solubility of retrotranslocated Hmg2-GFP. We first used the Usp2Core ubiquitin protease to remove the multiubiquitin from retrotranslocated Hmg2-GFP, and we tested its solubility; ultracentrifuged lysate with retrotranslocated Hmg2-GFP was treated with Usp2Core or buffer, followed by subsequent ultracentrifugation and analysis of its presence in the S100 or P100 fractions (Fig. 8*B*, *left*). An identical sample of retrotranslocated Hmg2-GFP was processed in reverse order; it was first ultracentrifuged and then Usp2Core-treated (Fig. 8*B*, *right*). Comparison of these two conditions showed that ubiquitinated Hmg2-GFP remained in the soluble fraction, whereas Hmg2-GFP that has been deubiquitinated with Usp2Core was rendered insoluble.

Removal of the ubiquitin chains from retrotranslocated Hmg2-GFP caused loss of both the covalently bound ubiquitin and the associated Cdc48, resulting in concomitant loss of Hmg2-GFP solubility. We next tested whether removal of only Cdc48 from retrotranslocated Hmg2-GFP would similarly affect solubility. Because the Cdc48 complex binds polyubiquitin chains, we tested the effect of adding commercially available free polyubiquitin chains on the association of Cdc48 with Hmg2-GFP and on the solubility of the retrotranslocated substrate. Direct addition of Lys-48-linked polyubiquitin (5 μM total Ub, 2–7 unit chain length) to the S100 supernatant for 1 h completely blocked the association of Cdc48 with retrotranslocated Hmg2-GFP as assessed by GFP-Trap coprecipitation (Fig. 9*A*). Furthermore, this treatment caused the Hmg2-GFP to become completely insoluble; after the same 1-h incubation with 5 μM polyubiquitin, the Hmg2-GFP was entirely pelleted by ultracentrifugation (Fig. 9*B*, *right*) but totally soluble in an identical experiment using buffer without added polyubiquitin (Fig. 9*B*, *left*).

During these polyubiquitin addition experiments, we noted a technical aspect that indicated a structural feature of retrotranslocated Hmg2-GFP. We found that the plastic centrifuge tubes used during the incubation required coating with BSA to prevent loss of the dislocated, soluble ubiquitinated Hmg2-GFP. If BSA coating was not included, the Cdc48-dissociated and ubiquitinated Hmg2-GFP was not recoverable from the pellet fraction (Fig. 9*B*, *right*). We interpreted this to mean that when the Cdc48 is removed by competition with the polyubiquitination, the resulting Hmg2-GFP is quite prone to interaction with hydrophobic surfaces such as unblocked plastic tube walls. This is reminiscent of the affinity that naked proteins show for untreated plastic that is so useful in solid state immunoassays (44). Although qualitative, the behavior of Hmg2-GFP when freed of Cdc48 is consistent with exposed hydrophobic regions that would be expected for an eight-spanning membrane protein wrested from this comfortable membrane roost.

Discussion

In this work we sought to discover the retrochaperones that allow multispanning membrane proteins to remain soluble after retrotranslocation during ERAD. Our initial buoyant density studies performed with our established *in vitro* ERAD assay showed that retrotranslocated, ubiquitinated Hmg2-GFP behaved like a purely proteinaceous complex, with no evidence of lipid involvement.

We developed a new *in vivo* retrotranslocation assay to ensure highest biological veracity; the *in vivo* assay showed two important features of regulated Hmg2 ERAD that were absent in the *in vitro* assay. First, Hmg2-GFP studied *in vivo* underwent normal regulation, responding to add GGPP, and allowed us to study and harness this aspect of Hmg2 degradation in these studies. Second, the effect of removing the homologous proteasome adaptors Dsk2 and Rad23 in the *in vivo* assay placed them in the expected position along the HRD pathway, after retrotranslocation and before proteasomal degradation. For reasons that are not clear, the *in vitro* assay's response to this double null blocks retrotranslocation (16). Retrotranslocated, ubiquitinated Hmg2-GFP observed *in vivo* was full length as indicated by proteolytic removal of ubiquitin. This was the case even for the ambient Hmg2-GFP found in the S100 fraction without inhibition of the proteasome or added GGPP signal, indicating that the retrotranslocation step was a normal

part of the ERAD-M process, and so it warranted detailed exploration.

Using the *in vivo* assay, we again tested the biophysical properties of retrotranslocated Hmg2-GFP to discern any role for lipids. This is particularly salient for Hmg2 because of an observed association between mammalian HMGR undergoing ERAD and lipid droplets in mammalian cells (29, 45). Nevertheless, it was clear that *in vivo* retrotranslocated Hmg2-GFP was entirely protein-associated. Similar recent studies on the misfolded, retrotranslocated Doa10 pathway substrate Ste6*-3HA reported that, unlike retrotranslocated Hmg2-GFP, Ste6*-3HA pelleted into the P100 fraction. When we performed our (very similar) protocol with Ste6*-3HA, it behaved identically to Hmg2-GFP, showing full solubility after retrotranslocation, remaining in S100. The nature of this discrepancy is not clear, but it could rest in minor differences in assay execution. Perhaps constitutively misfolded Ste6*-3HA is more prone to experimental aggregation, causing it to pellet upon ultracentrifugation, due to subtle differences in assay conditions. Whatever the explanation, our studies show striking commonality between these two types of integral membrane ERAD substrates, which was borne out by the subsequent proteomics and biochemistry.

We then used unbiased proteomics to identify and confirm Cdc48 as the principal retrochaperone allowing multispanning membrane proteins to remain soluble in the cytosol. Immunoprecipitation of retrotranslocated Hmg2 resulted in significant capture (~10% of the total pool) of free Cdc48. Importantly, clearance studies with fully functional ProtA-Cdc48 showed *all* of the retrotranslocated Hmg2-GFP were Cdc48-associated. Identical experiments with either Npl4 or Ufd1-SBP showed that soluble retrotranslocated Hmg2-GFP was entirely associated with the canonical Cdc48-Ufd1-Npl4 complex. Similarly, soluble retrotranslocated Ste6*-3HA was quantitatively associated with the Cdc48-Ufd1-Npl4 complex. Thus, this complex appears to be generally involved in both the ATP-dependent removal of ERAD-M substrates and maintenance of their solubility. A 2014 study implicates Cdc48 as solubilizing "holdase" for ubiquitinated substrates in the San1 nuclear quality control pathway (46), further extending the generality of this function. In interesting contrast to our observed need for the Cdc48-Ufd1-Npl4 in retrochaperone function, a new pathway for degradation of misfolded cytosolic proteins has been described that appears to employ a Cdc48-Npl4 subcomplex, with no involvement of Ufd1. Perhaps the Cdc48 complex composition allows mechanistic differences in use of the widely used quality control factor (47).

We explored the features of Cdc48-client interaction. The tripartite Cdc48 complex binds polyubiquitin chains. Proteolytic removal of the polyubiquitin from Hmg2-GFP abolished its Cdc48 association and rendered the retrotranslocated Hmg2-GFP insoluble. Similarly, addition of excess polyubiquitin chains to the assay supernatant resulted in complete loss of Cdc48 binding to retrotranslocated Hmg2-GFP, and again it caused drastic loss of Hmg2-GFP solubility. Thus, it was clear that polyubiquitin-mediated association of the Cdc48 complex is critical for the maintained solubility of the eight-spanning Hmg2-GFP, indicating that Cdc48 is a *bone fide* retrochaperone in addition to being a ubiquitin-dependent "dislocase."

The ability of added polyubiquitin chains to reverse Cdc48-client binding implies some interesting features of Cdc48 retrochaperone function. Cdc48/p97 has regions that could interact with hydrophobic portions of substrates (24, 48), so it was at least possible that inhibiting Cdc48 complex binding to polyubiquitin would still allow client association and solubility. That was not the case. The polyubiquitin binding of Cdc48 was a critical component of Cdc48 retrochaperone function. This could be due to simple avidity effects, such that the polyubiquitin provides stable association of Cdc48 in close proximity to weakly interacting hydrophobic portions of the substrate, thus allowing solubility. Alternatively, it is possible that a more complex interplay is involved. Perhaps polyubiquitin binding alters the Cdc48 complex, providing an allosteric contingency for Cdc48 interaction with hydrophobic clients. It will be important to test these and related ideas to understand this general function of Cdc48. The demonstrated requirement for polyubiquitin chains in Cdc48-mediated solubility also allows for a natural role for ubiquitin proteases in the transfer of the bound clients to proteasome adaptors or the proteasome itself. Because removal of the chains is sufficient to disengage Cdc48, the function of ERAD-important UBP (ubiquitin protease) such as Otu1 (49–51) may be to bring about disengagement by ubiquitin removal, thus allowing formation of distal substrate-adaptor complexes passed from Cdc48-substrate complexes upon ubiquitin removal.

It has been suggested that in ERAD-L the initial retrotranslocation of fully luminal substrates may be mediated by an intriguing, newly reported "ubiquitin-gated channel" activity of Hrd1 (18). By that model, the Hrd1 channel activity catalyzes transfer of the ERAD-L substrate to the ER surface, and Cdc48 then joins the process by binding to the ERAD-L substrate undergoing ubiquitination and retrotranslocation, providing further energy for transmembrane movement and solubilization. We asked if Cdc48 similarly had a "follow-through" role in HRD-dependent degradation of Hmg2. If so, we would expect Cdc48-deficient strains to show increased ER-associated ubiquitinated material on the outer surface of the ER, which would thus behave like an extrinsic membrane protein. In the wild-type strains, there is indeed a portion (about 10% of the total ubiquitinated Hmg2-GFP) that is found tightly bound on the surface of the ER, as indicated by its removal with pH 11.5 carbonate. However, in a *cdc48-2* strain, all of the ubiquitinated Hmg2-GFP was embedded in the membrane, behaving like an integral membrane protein. Thus, it appears that Cdc48 is important for the initial passage of ERAD-M substrates across the ER membrane, as well as the subsequent solubilization needed for transit to the proteasome.

It is interesting to compare the role of Cdc48 in yeast to the analogous pathways in the mammal. It is clear that p97, the mammalian homologue of Cdc48, is prominently featured in mammalian ERAD. However, the tail-anchor pathway protein Bag6, which is absent in yeast, also plays a role in a variety of quality control processes, including retrotranslocation, where it also acts as a cytoplasmic holdase (52). Current studies indicate that p97 and Bag6 may play parallel roles, because loss of

either causes slowing, but not complete loss, of ERAD substrate degradation (53). Intriguingly, Bag6's interaction with hydrophobic clients is not dependent on ubiquitination. This feature is appropriate considering Bag's better-studied role in promoting solubility of non-ubiquitinated cytoplasmic tail-anchored proteins. In fact, Bag6 may be able to recruit soluble E3s to promote ubiquitination of retrotranslocated substrates that have either not been ubiquitinated or have lost the modification (54). In contrast to mammals, retrotranslocated yeast substrates appear to always be ubiquitinated, whereas in the mammal both ubiquitinated and non-ubiquitinated forms of a given retrotranslocated substrate can sometimes be observed. One simple view of Bag6's role in ERAD is that perhaps in mammals there is a need for a parallel retrochaperone system for non-ubiquitinated ERAD substrates, because these would be invisible to the ubiquitin-dependent p97-Cdc48 complex. This added burden could be due to possible ubiquitin-independent pathways of retrotranslocation or to a greater propensity for mammalian cytosol to deubiquitinate retrotranslocated proteins. Perhaps there is an unknown fitness advantage to being able to process both ubiquitinated and non-ubiquitinated ERAD substrates, and so Bag6 was recruited for this added proteostatic function due to its fortuitous presence in the mammalian proteome. Whatever the evolutionary genesis of the Bag6 component of ERAD, it will be interesting and important to understand the integrated functions of these two complementary retrochaperones in mammalian ERAD.

Cdc48/p97 are AAA hexameric ATPases. They are thought to use ATP hydrolysis to generate the considerable conformational force needed for the many versions of ubiquitin-dependent extraction and dislocation for which they are well known (19). Especially in the case of ERAD-M retrotranslocation, prodigious energy would be required for substrate removal from the membrane. However, it is less clear if the retrochaperoning role of Cdc48 is also ATP-dependent. It will be important to evaluate the role of ATP in this novel holdase function, and a number of straightforward experiments are now possible with the assays and techniques developed herein.

Taken together, these studies show that the Cdc48 complex has a critical and general function as an "ERAD holdase" or retrochaperone. It has been clear for a number of years that Cdc48/p97 accompanies ERAD substrates on their way to the proteasome, but this work demonstrates that the solubility of the ubiquitinated substrates is only possible due to the chaperoning functions of the complex. There are both functional and pathological consequences of this critical new action. It will be intriguing to understand the mechanics and structural aspects of Cdc48 chaperoning and to eventually understand the breadth of this function in cellular processes, including both degradation and possible refolding of damaged proteins that engage the AAA-ATPases in the course of proteostasis.

Experimental Procedures

Yeast and Bacteria Growth Media—Standard yeast *S. cerevisiae* growth media were used as described previously (55), including yeast extract-peptone-dextrose (YPD) medium and ammonia-based synthetic complete dextrose (SC) and ammonia-based synthetic minimal dextrose (SD) medium supplemented with 2% dextrose and amino acids to enable growth of auxotrophic strains at 30 °C. *Escherichia coli* DH5 was grown in standard LB media with ampicillin at 37 °C, as described previously (56).

TABLE 2
Plasmids used in this study

Plasmid	Gene
pRH 469	YIp, URA3, pTDH3-HMG2-GFP
pRH 2695	YIp, URA3, pTDH3-GFP
pRH 1960	YCp, URA3, pCAU-KWW-3HA
pRH 373	YIp, TRP1, pTDH3-UBC7-2HA
pRH 2513	YIp, TRP1, pHRD1-5myc
pRH 2058	YCp, URA3, pPGK-STE6-166-3HA-GFP
pRH 2078	2μ, URA3, pNOPPA-ProA-CDC48

Plasmids and Strains—Plasmids used in this study are listed in Table 2. Plasmids for this work were generated using standard molecular biological techniques as described previously (57) and verified by sequencing (Eton Bioscience, Inc.). Primer information is available upon request. The KWW (pRH1960) plasmid was a gift from Davis Ng (National University of Singapore, Singapore). The protein A-CDC48 (pRH2078) plasmid was a gift from M. Latterich (McGill University, Quebec, Canada). The Ste6* plasmid (pRH2058) was a gift from S. Michaelis (The Johns Hopkins School of Medicine, Baltimore, MD).

A complete list of yeast strains and their corresponding genotypes are compiled in Table 3. The UFD1-SBP strain was a gift from T. Rapoport (Harvard Medical School, MA). All strains used in this work were derived from S288C. Yeast strains were transformed with DNA or PCR fragments using the standard LiOAc method (32). Null alleles were generated by using PCR to amplify a selection marker flanked by 50 base pairs of the 5′ and 3′ regions, which are immediately adjacent to the coding region of the gene to be deleted. The selectable markers used for making null alleles were the *LEU2* gene (amplified from pRS405) or genes encoding resistance to G418 or CloNat/nourseothricin. After transformation, strains with drug markers were plated onto YPD followed by replica-plating onto YPD plates containing (500 μg/ml G418 or 200 μg/ml nourseothricin). All gene deletions were confirmed by PCR. The CDC48 coding region was replaced *in situ* with the fusion coding region for protein A (ProtA)-Cdc48 by homologous recombination with two cotransformed PCR products. These products were amplified from plasmid pRH2078, which has a cloned genomic fragment bearing the ProtA-Cdc48 allele in the normal CDC48 locus. The first PCR product consisted of the 5′ promoter region, the ProtA-Cdc48 coding region, the 3′ terminator region and the 5′ end of a nourseothricin expression cassette. The second PCR product consisted of the complete nourseothricin expression cassette followed by the 3′-flanking region of the CDC48 locus. Cotransformation of a native yeast strain with both products resulted in replacement of the native Cdc48 coding region with that of ProtA-Cdc48, followed by a nourseothricin expression cassette allowing selection for successful replacement. Cotransformed cells were selected for nourseothricin resistance, confirmed by PCR, and tested by immunoblotting for ProtA-Cdc48 as the only version of Cdc48 expressed. Primer sequences are available upon request.

In Vitro Ubiquitination Assay—Ubiquitination of Hmg2-GFP was prepared and analyzed as described previously (16). Briefly,

TABLE 3
Yeast strains used in this study

Strain	Genotype	Refs.
RHY 4288	Matα *ade2-101 met2 lys2-801 his3Δ200 trp1::hisG leu2Δ ura3-52 pep4Δ::HIS3 hmg2Δ::1myc-HMG2 hrd1Δ::kanMX ubc7Δ::LEU2*	16
RHY 4295	Matα *ade2-101 met2 lys2-801 his3Δ200 trp1::hisG::TRP1::TDH3$_{prom}$ -UBC7-2HA leu2Δ ura3-52 pep4Δ::HIS3 hmg2Δ::1myc-HMG2 hrd1Δ::kanMX ubc7Δ::LEU2*	16
RHY 2923	Matα *ade2-101 met2 lys2-801 his3Δ200 trp1::hisG::TRP1::TDH3$_{prom}$ -Hrd1-3HA leu2Δ ura3-52::URA3::TDH3$_{prom}$ -HMG2-GFP pep4Δ::HIS3 hmg2Δ::1myc-HMG2 hrd1Δ::kanMX ubc7Δ::LEU2*	16
RHY 5550	Matα *ade2-101 met2 lys2-801 his3Δ200 trp1::hisG::TRP1::TDH3$_{prom}$ -HRD1-3HA leu2Δ Ura3-52::URA3::TDH3$_{prom}$ -HMG2-GFP pep4Δ::HIS3 hmg2Δ::1myc-HMG2 hrd1Δ::kanMX ubc7Δ::LEU2 cdc48-2::NatR*	16
RHY 5551	Matα *ade2-101 met2 lys2-801 his3Δ200 trp1::hisG::TRP1::TDH3$_{prom}$ -UBC7-2HA leu2Δ ura3-52::URA3::TDH3$_{prom}$ -HMG2-GFP pep4Δ::HIS3 hmg2Δ::1myc-HMG2 hrd1Δ::kanMX ubc7Δ::LEU2 cdc48-2::NatR*	16
RHY 8073	Mata *ade2-101 met2 lys2-801 his3Δ200 trp1::hisG leu2Δ ura3-52::URA3::TDH3prom-Hmg2-GFP pdr5Δ::kanMX*	This study
RHY 10791	Mata *ade2-101 met2 lys2-801 his3Δ200 trp1::hisG leu2Δ ura3-52::TDH3$_{prom}$ -GFP pdr5Δ::kanMX*	This study
RHY 9925	Mata *ade2-101 met2 lys2-801 his3Δ200 trp1::hisG leu2Δ ura3-52::URA3::TDH3$_{prom}$ -Hmg2-GFP cdc48-2::NatR pdr5Δ::LEU2*	This study
RHY 9926	Matα *ade2-101 met2 lys2-801 his3Δ200 trp1::hisG leu2Δ ura3-52::URA3::TDH3$_{prom}$ -Hmg2-GFP pdr5Δ::LEU2 hrd2-1*	This study
RHY 5804	Mata *ade2-101 met2 lys2-801 his3Δ200 trp1::hisG leu2Δ ura3-52::URA3::TDH3$_{prom}$ -Hmg2-GFP dsk2Δ::kanMX rad23Δ::NatR*	58
RHY 9136	Mata *ade2-101 met2 lys2-801 his3Δ200 trp1::hisG::TRP1::pHrd1–5myc leu2Δ ura3-52*	59
RHY 8408	Mata *ade2-101 met2 lys2-801 his3Δ200 trp1::hisG leu2Δ ura3-52 pdr5Δ::LEU2 CEN::URA3::CAU$_{prom}$ -KWW-3Ha*	58
RHY5389	Mata *ade2-101 met2 lys2-801 his3Δ200 trp1::hisG leu2Δ ura3-52 2μ::URA3:: PGK$_{prom}$ -Ste6-166-3Ha-GFP*	58
RHY10649	Mata *ade2-101 met2 lys2-801 his3Δ200 trp1::hisG leu2Δ ura3-52::URA3::TDH3$_{prom}$ -Hmg2-GFP cdc48Δ::NatR:: NOPPA$_{prom}$ -ProA-CDC48 pdr5Δ::kanMX*	This study
RHY10650	Mata *ade2-101 met2 lys2-801 his3Δ200 trp1::hisG leu2Δ ura3-52 cdc48Δ::NatR::NOPPA$_{prom}$ -ProA-CDC48 2μ:: URA3::PGK$_{prom}$ -Ste6-166-3Ha-GFP pdr5Δ::kanMX*	This study
RHY10789	Mat a ADE2:: URA3:: *TDH3$_{prom}$ -Hmg2-GFP met15Δ his3Δ1 leu2Δ0 ura3Δ0 pdr5Δ::NatR ufd1Δ::HphMX4::UFD1-SBP*	This study
RHY10790	Mat a *met15Δ his3Δ1 leu2Δ0 ura3Δ0 pdr5Δ::NatR ufd1Δ::HphMX4::UFD1-SBP 2μ::URA3::PGK$_{prom}$ -Ste6-166-3Ha-GFP*	This study

cytosols from strains overexpressing Ubc7 or an otherwise identical *ubc7*Δ null strain were lysed by grinding under liquid nitrogen and ultracentrifuged for membrane removal. Protein concentrations were measured by NanoDrop (Thermo Fisher Scientific). Cytosol concentrations were adjusted to 20–25 mg/ml for ubiquitination and retrotranslocation assays. Microsomes were prepared from *ubc7*Δ null yeast strain expressing 3HA-Hrd1 and Hmg2-GFP by bead lysis followed by membrane fractionation. The microsomal pellets were resuspended in the same buffer used to prepare cytosol. One *in vitro* ubiquitination reaction consisted of 10 μl of microsome and 12 μl of cytosol. ATP was added to each reaction to a final concentration of 30 mM to initiate reaction, and the reaction was then incubated for 1 h at 30 °C. The assay was solubilized in 200 μl of SUME (1% SDS, 8 M urea, 10 mM MOPS, pH 6.8, 10 mM EDTA) with protease inhibitors and 5 mM *N*-ethylmaleimide (NEM). Detergent immunoprecipitation buffer (IPB) was added followed by addition of 15 μl of rabbit polyclonal anti-GFP antisera (C. Zuker, University of California, San Diego) for immunoprecipitation (IP) of Hmg2-GFP. Samples were incubated on ice for 5 min, clarified at 14,000 × *g* for 5 min, and removed to a new Eppendorf tube and incubated overnight at 4 °C. 100 μl of equilibrated protein A-Sepharose in IPB (50% w/v) (Amersham Biosciences) was added and incubated for 2 h at 4 °C. Proteins A beads were washed twice with IPB and washed once more with IP wash buffer (50 mM NaCl, 10 mM Tris), aspirated to dryness, resuspended in 2× urea sample buffer (2× USB: 8 M urea, 4% SDS, 1 mM DTT, 125 mM Tris, pH 6.8), and incubated at 55 °C for 10 min. IPs were resolved by 8% SDS-PAGE, transferred to nitrocellulose, and immunoblotted with monoclonal anti-ubiquitin (Fred Hutchinson Cancer Center, Seattle) and anti-GFP (Clontech). Goat anti-mouse (Jackson ImmunoResearch, West Grove, PA) and goat anti-rabbit (Bio-Rad) conjugated with horseradish peroxidase (HRP) recognized primary antibodies. Western Lightning® Plus (PerkinElmer Life Sciences) chemiluminescence reagents were used for immunodetection.

In Vitro Retrotranslocation Assay—In vitro retrotranslocation assay of Hmg2-GFP was performed as described previously (16). Briefly, each *in vitro* retrotranslocation set of total, supernatant, and pellet fractions was derived from 3× *in vitro* ubiquitination reaction. The reaction proceeded at 30 °C for 1 h, and one reaction equivalent (25 μl) was transferred to tube designated as total and another reaction equivalent was transferred to a tube for centrifugation for 1 h at 25,000 × *g* at 4 °C. The resulting supernatant (S) was carefully removed, and the resulting P was resuspended in the same volume as the supernatant and total fractions. Each fraction was solubilized with SUME with PIs + NEM and immunoprecipitated and detected as described above for *in vitro* ubiquitination assay.

Drug Treatment—Where indicated, log phase cultures were treated with MG132 (benzyloxycarbonyl-Leu-Leu-aldehyde, Sigma) at a final concentration of 25 μg/ml (25 mg/ml stock dissolved in DMSO) for 2 h at 30 °C and/or GGPP ammonium salt (Sigma) at a final concentration of 11 μM for 1 h at 30 °C.

In Vivo Retrotranslocation Assay—In vivo retrotranslocation assay was adapted and modified from Ref. 30. Cells in log phase (OD_{600} 0.2–0.3) were treated with MG132 and GGPP, and 15 ODs of cells were pelleted. Cells were resuspended in H_2O, centrifuged, and lysed by with the addition of 0.5 mM glass beads and 400 μl of diluted XL buffer (0.24 M sorbitol, 1 mM EDTA, 20 mM KH_2PO_4, final pH 7.5) with PIs, followed by vortexing in 1-min intervals for 6–8 min at 4 °C. Lysates were combined and clarified by centrifugation at 2,500 × *g* for 5 min. Clarified lysate was ultracentrifuged at 100,000 × *g* for 15 min to separate pellet (P100) and supernatant fraction (S100). P100 pellet was resuspended in 200 μl of SUME with PIs and NEM followed by addition of 600 μl of IPB with PIs and NEM. S100 supernatant was added directly to IPB with PIs, and NEM and IP for both P100 and S100 were carried out as described above for *in vitro* ubiquitination assay. 30 and 5 μl of IP were used for detection of ubiquitinated Hmg2-GFP with anti-ubiquitin and detection of Hmg2-GFP with anti-GFP, respectively.

Proteolytic Removal of Ubiquitin from Retrotranslocated Hmg2-GFP—Ubiquitin removal was accomplished with the broadly active Usp2 ubiquitin protease as described previously

(16), except that human recombinant Usp2Core (LifeSensors Inc., Malvern, PA) was used, and leupeptin and NEM were excluded from all buffers. Briefly, 50 μl of S100 supernatant containing retrotranslocated Hmg2-GFP was incubated with 10 μl of Usp2Core (5 μg) for 1 h at 37 °C. The reaction was quenched with 200 μl of SUME with PIs, and retrotranslocated Hmg2-GFP was immunoprecipitated as described above. 20 μl of IP was used for detection of Hmg2-GFP with anti-GFP.

Ultracentrifugal Flotation Assay—The sucrose density flotation assay was modified from Ref. 10. S20 supernatant from *in vitro* retrotranslocation assay or S100 supernatant from *in vivo* retrotranslocation assay was isolated as described above except MSB buffer (50 mM HEPES, 150 mM NaCl, 5 mM EDTA, pH 7.6) was used instead of diluted XL buffer. 100 μl of lysate or supernatant fraction containing retrotranslocated Hmg2-GFP was mixed with 300 μl of MSB containing 2.3 M sucrose, and this solution was layered onto 200 μl of MSB containing 2.3 M sucrose in a centrifuge tube. MSB supplemented with 1.5 M sucrose (500 μl) and 0.25 M sucrose (400 μl) were successively layered, and the tube was centrifuged in a Beckman SW55 rotor at 100,00 × *g* for 16 h at 4 °C. Fractions of 100 μl were removed from the top of the gradient. For analysis of PGK and Sec61, each fraction was mixed with 2× USB, resolved by SDS-PAGE, and immunoblotted with monoclonal antibodies anti-Sec61 (Randy Schekman's laboratory) and anti-PGK (Life Technologies, Inc.-Novex). For analysis of retrotranslocated Hmg2-GFP, each fraction was immunoprecipitated and immunoblotted as described above for *in vitro* ubiquitination assay.

Carbonate Extraction—Carbonate extraction was modified from Ref. 37. Briefly, 200 μg of microsomes were incubated in 200 μl of 0.2 M Na_2CO_3 at the indicated pH value for 15 min on ice. Samples were centrifuged at 14,000 × *g* for 10 min to separate the P and S. Supernatants were precipitated with 20% (w/v) TCA, and both the pellet and supernatant fractions were resuspended in equal volumes of 2× USB buffer. For analysis of ubiquitinated Hmg2-GFP, following treatment with Na_2CO_3 at pH 11.5 and centrifugation, the pellet fraction was resuspended in 200 μl of SUME with PIs and NEM followed by addition of 600 μl of IPB with PIs and NEM, whereas the supernatant fraction was added directly to IPB with PIs and NEM. IP for both pellet and supernatant fraction was carried out as described above for *in vitro* ubiquitination assay.

Co-IP of Retrotranslocated Hmg2-GFP for Mass Spectrometry Analysis—Log phase cultures (OD_{600} 0.2–0.45) were treated with both MG132 and GGPP, and 30 ODs of cells were pelleted, rinsed with H_2O, and lysed with 0.5 mM glass beads in 800 μl of XL buffer with PIs (for mass spectrometry analyses, 4-(2-aminoethyl)benzenesulfonyl fluoride and NEM were excluded from all buffers). This was followed by vortexing at 1-min intervals for 6–8 min at 4 °C. Lysates were combined and clarified by centrifugation at 2,500 × *g* for 5 min followed by ultracentrifugation at 100,000 × *g* for 15 min to separate P100 pellet and S100 supernatant. 600 μl of S100 supernatant was divided and aliquoted into three tubes (200 μl per tube) containing non-detergent IP buffer (15 mM Na_2HPO_4, 150 mM NaCl, 10 mM EDTA) with PIs. Samples were incubated overnight with 10 μl of equilibrated GFP-Trap®-agarose (ChromoTek Inc., Hauppauge, NY) at 4 °C. The next day, GFP-Trap®-agarose beads were combined to one tube, washed once with non-detergent IP buffer, washed once more with IP wash buffer, and aspirated to dryness. Beads were resuspended in 50 μl of 0.2 M glycine, pH 2.5, followed by addition of 5 μl of 1 M Tris base, pH 10.4, for neutralization. Neutralized sample was then subjected for mass spectrometry analysis.

Clearance Assay—Strains expressing Hmg2-GFP and ProtA-Cdc48 as the only source of Cdc48 were grown to log phase and subjected to the *in vivo* retrotranslocation assay preparation of S100, but with leupeptin and NEM excluded from all buffers. Following ultracentrifugation, 200 μl of each S100 supernatant fraction was added to tubes containing 600 μl of non-detergent IP buffer with PIs, clarified by 21,000 × *g* spin for 10 min, transferred to new tubes, followed by addition of 70 μl of equilibrated IgG-Sepharose to each. Tubes were nutated overnight at 4 °C. The IgG-Sepharose was then washed once with non-detergent IP buffer, washed once more with IP wash buffer, and aspirated to dryness. Beads were resuspended in 50 μl of XL buffer supplemented with PIs, and 5 μl of Usp2Core (2.5 μg) was added to each tube followed by incubation for 1 h at 37 °C to allow removal of the ubiquitin attached to Hmg2-GFP to facilitate immunodetection (see above). After incubation, the reaction was quenched with 50 μl of 2× USB buffer. IPs were resolved by SDS-PAGE using 8% gels and immunoblotted with polyclonal antibody anti-Cdc48 for detection of ProtA-Cdc48 and anti-GFP for detection of Hmg2-GFP.

Solubility Assay—S100 supernatant containing retrotranslocated Hmg2-GFP was isolated as described above for *in vivo* retrotranslocation assay except that leupeptin and NEM were excluded from all buffers. For discerning solubility of ubiquitinated Hmg2-GFP, 200 μl of S100 supernatant was ultracentrifuged at 100,000 × *g* for 15 min. The pellet fraction obtained from this spin was resuspended in 200 μl of XL buffer with PIs. 5 μg of Usp2Core was added to both pellet and supernatant fractions and incubated for 1 h at 37 °C.

For discerning solubility of deubiquitinated Hmg2-GFP, 200 μl of S100 supernatant was treated with 10 μl (5 μg) of Usp2Core, incubated for 1 h at 37 °C, and ultracentrifuged at 100,000 × *g* for 15 min. The resulting pellet fraction was resuspended in XL buffer containing PIs. IP and anti-GFP immunoblotting for Hmg2-GFP from both pellet and supernatant fraction were carried out as described above for *in vitro* ubiquitination assay, and 20 and 40 μl of IP were used for detection of ubiquitin with anti-ubiquitin and detection of Hmg2-GFP with anti-GFP, respectively.

Free Polyubiquitin Competition Test—The ability of polyubiquitin to compete for Cdc48 binding to retrotranslocated Hmg2-GFP was adapted from Co-IP of retrotranslocated Hmg2-GFP as described above. S100 supernatant prepared according to the *in vivo* retrotranslocation assay above (total volume 600 μl), containing retrotranslocated Hmg2-GFP, was incubated with 10 μl (20 μg) of Lys-48-linked polyubiquitin chains (BostonBiochem®) or buffer for 1 h at room temperature. The incubation mixture was next distributed as 200-μl samples into three Eppendorf tubes containing 600 μl of non-detergent IP buffer with PIs. 10 μl of equilibrated GFP-Trap®-agarose was added to each tube, and they were nutated overnight at 4 °C. The next day, the GFP-Trap®-agarose beads were

combined to one tube, washed once with non-detergent IP buffer, washed once more with IP wash buffer, and resuspended in 100 μl of 2× USB. Samples were resolved on 8% SDS-PAGE and immunoblotted for ubiquitin and Cdc48.

Author Contributions—S. N. and R. H. designed the study, wrote the manuscript, and critically analyzed all the data. S. N. conducted all the experiments. R. M. and E. J. B. processed and analyzed samples for mass spectrometry analysis. All authors reviewed the results and approved the final version of the manuscript.

Acknowledgments—We thank Davis Ng (National University of Singapore), Randy Schekman (University of California, Berkeley), and Susan Michaelis (The Johns Hopkins University) for providing plasmids and antibodies. We also thank the Hampton laboratory members for discussions and technical assistance.

References

1. Foresti, O., Ruggiano, A., Hannibal-Bach, H. K., Ejsing, C. S., and Carvalho, P. (2013) Sterol homeostasis requires regulated degradation of squalene monooxygenase by the ubiquitin ligase Doa10/Teb4. *Elife* **2,** e00953
2. Hampton, R. Y., and Garza, R. M. (2009) Protein quality control as a strategy for cellular regulation: lessons from ubiquitin-mediated regulation of the sterol pathway. *Chem. Rev.* **109,** 1561–1574
3. Bays, N. W., Gardner, R. G., Seelig, L. P., Joazeiro, C. A., and Hampton, R. Y. (2001) Hrd1p/Der3p is a membrane-anchored ubiquitin ligase required for ER-associated degradation. *Nat. Cell Biol.* **3,** 24–29
4. Chen, B., Mariano, J., Tsai, Y. C., Chan, A. H., Cohen, M., and Weissman, A. M. (2006) The activity of a human endoplasmic reticulum-associated degradation E3, gp78, requires its Cue domain, RING finger, and an E2-binding site. *Proc. Natl. Acad. Sci. U.S.A.* **103,** 341–346
5. Swanson, R., Locher, M., and Hochstrasser, M. (2001) A conserved ubiquitin ligase of the nuclear envelope/endoplasmic reticulum that functions in both ER-associated and Matα2 repressor degradation. *Genes Dev.* **15,** 2660–2674
6. Richly, H., Rape, M., Braun, S., Rumpf, S., Hoege, C., and Jentsch, S. (2005) A series of ubiquitin binding factors connects CDC48/p97 to substrate multiubiquitylation and proteasomal targeting. *Cell* **120,** 73–84
7. Plemper, R. K., Egner, R., Kuchler, K., and Wolf, D. H. (1998) Endoplasmic reticulum degradation of a mutated ATP-binding cassette transporter Pdr5 proceeds in a concerted action of Sec61 and the proteasome. *J. Biol. Chem.* **273,** 32848–32856
8. Vashist, S., and Ng, D. T. (2004) Misfolded proteins are sorted by a sequential checkpoint mechanism of ER quality control. *J. Cell Biol.* **165,** 41–52
9. Jo, Y., and Debose-Boyd, R. A. (2010) Control of cholesterol synthesis through regulated ER-associated degradation of HMG CoA reductase. *Crit. Rev. Biochem. Mol. Biol.* **45,** 185–198
10. Zhang, Y., Nijbroek, G., Sullivan, M. L., McCracken, A. A., Watkins, S. C., Michaelis, S., and Brodsky, J. L. (2001) Hsp70 molecular chaperone facilitates endoplasmic reticulum-associated protein degradation of cystic fibrosis transmembrane conductance regulator in yeast. *Mol. Biol. Cell* **12,** 1303–1314
11. Carvalho, P., Goder, V., and Rapoport, T. A. (2006) Distinct ubiquitin-ligase complexes define convergent pathways for the degradation of ER proteins. *Cell* **126,** 361–373
12. Bordallo, J., Plemper, R. K., Finger, A., and Wolf, D. H. (1998) Der3p/Hrd1p is required for endoplasmic reticulum-associated degradation of misfolded luminal and integral membrane proteins. *Mol. Biol. Cell.* **9,** 209–222
13. Hampton, R. Y., Gardner, R. G., and Rine, J. (1996) Role of 26S proteasome and HRD genes in the degradation of 3-hydroxy-3-methylglutaryl-CoA reductase, an integral endoplasmic reticulum membrane protein. *Mol. Biol. Cell.* **7,** 2029–2044
14. Hampton, R. Y., and Sommer, T. (2012) Finding the will and the way of ERAD substrate retrotranslocation. *Curr. Opin. Cell Biol.* **24,** 460–466
15. Hiller, M. M., Finger, A., Schweiger, M., and Wolf, D. H. (1996) ER degradation of a misfolded luminal protein by the cytosolic ubiquitin-proteasome pathway. *Science* **273,** 1725–1728
16. Garza, R. M., Sato, B. K., and Hampton, R. Y. (2009) *In vitro* analysis of Hrd1p-mediated retrotranslocation of its multispanning membrane substrate 3-hydroxy-3-methylglutaryl (HMG)-CoA reductase. *J. Biol. Chem.* **284,** 14710–14722
17. Nakatsukasa, K., Huyer, G., Michaelis, S., and Brodsky, J. L. (2008) Dissecting the ER-associated degradation of a misfolded polytopic membrane protein. *Cell* **132,** 101–112
18. Baldridge, R. D., and Rapoport, T. A. (2016) Autoubiquitination of the Hrd1 ligase triggers protein retrotranslocation in ERAD. *Cell* **166,** 394–407
19. Xia, D., Tang, W. K., and Ye, Y. (2016) Structure and function of the AAA+ ATPase p97/Cdc48p. *Gene* **583,** 64–77
20. Braun, S., Matuschewski, K., Rape, M., Thoms, S., and Jentsch, S. (2002) Role of the ubiquitin-selective CDC48(UFD1/NPL4)chaperone (segregase) in ERAD of OLE1 and other substrates. *EMBO J.* **21,** 615–621
21. Meyer, H. H., Shorter, J. G., Seemann, J., Pappin, D., and Warren, G. (2000) A complex of mammalian ufd1 and npl4 links the AAA-ATPase, p97, to ubiquitin and nuclear transport pathways. *EMBO J.* **19,** 2181–2192
22. Bays, N. W., Wilhovsky, S. K., Goradia, A., Hodgkiss-Harlow, K., and Hampton, R. Y. (2001) HRD4/NPL4 is required for the proteasomal processing of ubiquitinated ER proteins. *Mol. Biol. Cell.* **12,** 4114–4128
23. Pye, V. E., Dreveny, I., Briggs, L. C., Sands, C., Beuron, F., Zhang, X., and Freemont, P. S. (2006) Going through the motions: the ATPase cycle of p97. *J. Struct. Biol.* **156,** 12–28
24. Ye, Y., Meyer, H. H., and Rapoport, T. A. (2003) Function of the p97-Ufd1-Npl4 complex in retrotranslocation from the ER to the cytosol: dual recognition of nonubiquitinated polypeptide segments and polyubiquitin chains. *J. Cell Biol.* 077114:21–9525,
25. Balch, W. E., Morimoto, R. I., Dillin, A., and Kelly, J. W. (2008) Adapting proteostasis for disease intervention. *Science* **319,** 916–919
26. Vangala, J. R., Sotzny, F., Krüger, E., Deshaies, R. J., and Radhakrishnan, S. K. (2016) Nrf1 can be processed and activated in a proteasome-independent manner. *Curr. Biol.* **26,** R834–R835
27. Nakatsukasa, K., and Kamura, T. (2016) Subcellular fractionation analysis of the extraction of ubiquitinated polytopic membrane substrate during ER-associated degradation. *PLoS ONE* **11,** e0148327
28. Ploegh, H. L. (2007) A lipid-based model for the creation of an escape hatch from the endoplasmic reticulum. *Nature* **448,** 435–438
29. Hartman, I. Z., Liu, P., Zehmer, J. K., Luby-Phelps, K., Jo, Y., Anderson, R. G., and DeBose-Boyd, R. A. (2010) Sterol-induced dislocation of 3-hydroxy-3-methylglutaryl coenzyme A reductase from endoplasmic reticulum membranes into the cytosol through a subcellular compartment resembling lipid droplets. *J. Biol. Chem.* **285,** 19288–19298
30. Jarosch, E., Taxis, C., Volkwein, C., Bordallo, J., Finley, D., Wolf, D. H., and Sommer, T. (2002) Protein dislocation from the ER requires polyubiquitination and the AAA-ATPase Cdc48. *Nat. Cell Biol.* **4,** 134–139
31. Garza, R. M., Tran, P. N., and Hampton, R. Y. (2009) Geranylgeranyl pyrophosphate is a potent regulator of HRD-dependent 3-hydroxy-3-methylglutaryl-CoA reductase degradation in yeast. *J. Biol. Chem.* **284,** 35368–35380
32. Ito, H., Fukuda, Y., Murata, K., and Kimura, A. (1983) Transformation of intact yeast cells treated with alkali cations. *J. Bacteriol.* **153,** 163–168
33. Rao, H., and Sastry, A. (2002) Recognition of specific ubiquitin conjugates is important for the proteolytic functions of the ubiquitin-associated domain proteins Dsk2 and Rad23. *J. Biol. Chem.* **277,** 11691–11695
34. Wilkinson, C. R., Seeger, M., Hartmann-Petersen, R., Stone, M., Wallace, M., Semple, C., and Gordon, C. (2001) Proteins containing the UBA domain are able to bind to multi-ubiquitin chains. *Nat. Cell Biol.* **3,** 939–943
35. Ye, Y., Meyer, H. H., and Rapoport, T. A. (2001) The AAA ATPase Cdc48/p97 and its partners transport proteins from the ER into the cytosol. *Nature* **414,** 652–656
36. Doolman, R., Leichner, G. S., Avner, R., and Roitelman, J. (2004) Ubiquitin is conjugated by membrane ubiquitin ligase to three sites, including the N terminus, in transmembrane region of mammalian 3-hydroxy-3-methyl-

glutaryl coenzyme A reductase: implications for sterol-regulated enzyme degradation. *J. Biol. Chem.* **279,** 38184–38193
37. Claypool, S. M., McCaffery, J. M., and Koehler, C. M. (2006) Mitochondrial mislocalization and altered assembly of a cluster of Barth syndrome mutant tafazzins. *J. Cell Biol.* **174,** 379–390
38. Mateja, A., Paduch, M., Chang, H.-Y., Szydlowska, A., Kossiakoff, A. A., Hegde, R. S., and Keenan, R. J. (2015) Protein targeting. Structure of the Get3 targeting factor in complex with its membrane protein cargo. *Science* **347,** 1152–1155
39. Flierman, D., Ye, Y., Dai, M., Chau, V., and Rapoport, T. A. (2003) Polyubiquitin serves as a recognition signal, rather than a ratcheting molecule, during retrotranslocation of proteins across the endoplasmic reticulum membrane. *J. Biol. Chem.* **278,** 34774–34782
40. Pye, V. E., Beuron, F., Keetch, C. A., McKeown, C., Robinson, C. V., Meyer, H. H., Zhang, X., and Freemont, P. S. (2007) Structural insights into the p97-Ufd1-Npl4 complex. *Proc. Natl. Acad. Sci. U.S.A.* **104,** 467–472
41. Wu, X., Li, L., and Jiang, H. (2016) Doa1 targets ubiquitinated substrates for mitochondria-associated degradation. *J. Cell Biol.* **213,** 49–63
42. Ramadan, K., Bruderer, R., Spiga, F. M., Popp, O., Baur, T., Gotta, M., and Meyer, H. H. (2007) Cdc48/p97 promotes reformation of the nucleus by extracting the kinase Aurora B from chromatin. *Nature* **450,** 1258–1262
43. Wilcox, A. J., and Laney, J. D. (2009) A ubiquitin-selective AAA-ATPase mediates transcriptional switching by remodelling a repressor-promoter DNA complex. *Nat. Cell Biol.* **11,** 1481–1486
44. Catt, K., and Tregear, G. W. (1967) Solid-phase radioimmunoassay in antibody-coated tubes. *Science* **158,** 1570–1572
45. Jo, Y., Hartman, I. Z., and DeBose-Boyd, R. A. (2013) Ancient ubiquitous protein-1 mediates sterol-induced ubiquitination of 3-hydroxy-3-methylglutaryl CoA reductase in lipid droplet-associated endoplasmic reticulum membranes. *Mol. Biol. Cell.* **24,** 169–183
46. Gallagher, P. S., Clowes Candadai, S. V., and Gardner, R. G. (2014) The requirement for Cdc48/p97 in nuclear protein quality control degradation depends on the substrate and correlates with substrate insolubility. *J. Cell Sci.* **127,** 1980–1991
47. Xu, Y., Anderson, D. E., and Ye, Y. (2016) The HECT domain ubiquitin ligase HUWE1 targets unassembled soluble proteins for degradation. *Cell Discov.* **2,** 16040
48. Song, C., Wang, Q., and Li, C. C. (2007) Characterization of the aggregation-prevention activity of p97/valosin-containing protein. *Biochemistry* **46,** 14889–14898
49. Stein, A., Ruggiano, A., Carvalho, P., and Rapoport, T. (2014) Key steps in ERAD of luminal ER proteins reconstituted with purified components. *Cell* **158,** 1375–1388
50. Finley, D. (2009) Recognition and processing of ubiquitin-protein conjugates by the proteasome. *Annu. Rev. Biochem.* **78,** 477–513
51. Ernst, R., Mueller, B., Ploegh, H. L., and Schlieker, C. (2009) The otubain YOD1 is a deubiquitinating enzyme that associates with p97 to facilitate protein dislocation from the ER. *Mol. Cell* **36,** 28–38
52. Casson, J., McKenna, M., and High, S. (2016) On the road to nowhere: cross-talk between post-translational protein targeting and cytosolic quality control. *Biochem. Soc. Trans.* **44,** 796–801
53. Zhang, T., Xu, Y., Liu, Y., and Ye, Y. (2015) gp78 functions downstream of Hrd1 to promote degradation of misfolded proteins of the endoplasmic reticulum. *Mol. Biol. Cell* **26,** 4438–4450
54. Rodrigo-Brenni, M. C., Gutierrez, E., and Hegde, R. S. (2014) Cytosolic quality control of mislocalized proteins requires RNF126 recruitment to Bag6. *Mol. Cell.* **55,** 227–237
55. Hampton, R. Y., and Rine, J. (1994) Regulated degradation of HMG-CoA reductase, an integral membrane protein of the endoplasmic reticulum, in yeast. *J. Cell Biol.* **125,** 299–312
56. Gardner, R., Cronin, S., Leader, B., Rine, J., Hampton, R., and Leder, B. (1998) Sequence determinants for regulated degradation of yeast 3-hydroxy-3-methylglutaryl-CoA reductase, an integral endoplasmic reticulum membrane protein. *Mol. Biol. Cell* **9,** 2611–2626
57. Sato, B. K., Schulz, D., Do, P. H., and Hampton, R. Y. (2009) Misfolded membrane proteins are specifically recognized by the transmembrane domain of the Hrd1p ubiquitin ligase. *Mol. Cell* **34,** 212–222
58. Sato, B., K., and Hampton, R. Y. (2006) Yeast Derlin Dfm1 interacts with Cdc48 and functions in ER homeostasis. *Yeast* 10.1002/yea.1407
59. Vashistha, N., Neal, S. E., Singh, A., Carroll, S. M., and Hampton, R. Y. (2016) Direct and essential function for Hrd3 in ER-associated degradation. *Proc. Natl. Acad. Sci. U.S.A.* **113,** 5934–5939